

PETROLEUM REPORT SERIES

PR4882

Title **Late Miocene surface heat flow and thermal modelling of Murchison and southern Taranaki basins, New Zealand**

Operator

Author S.Lee, P.J.J. Kamp and K.P. Furlong

Date 2014

Summary Numerical thermal modelling of the successions intersected in Fresne-1, North Tasman-1 and Surville-1, southern Taranaki Basin, establishes a Late Miocene surface heat flow value of 77 ± 6 mWm⁻² compared with a present-day value of 70 ± 12 mWm⁻². This analysis relies upon 2700 m of Late Miocene – Pliocene erosion at Fresne-1, established by seismic reflection mapping. The use of this Late Miocene surface heat flow value in thermal modelling of the succession in Bounty-1 together with apatite fission track data, establishes a 10 Ma timing for the start of uplift and an c. 8 Ma timing for the start of erosion of the 2700 m of the sedimentary section that formerly overlay the top of the Bounty-1 succession. Murchison and southern Taranaki basins had similar timing (Late Miocene) and duration of hydrocarbon maturation prior to the start of Basin inversion.

This report has been compiled from material submitted to the New Zealand Government under legislation or voluntarily by exploration companies. An acknowledgement of this work in the following bibliographic format would be appreciated:

Lee, S., Kamp, P.J.J., Furlong, K.P. 2013: Late Miocene surface heat flow and thermal modelling of Murchison and southern Taranaki basins, New Zealand Ministry of Business, Innovation and Employment, New Zealand, unpublished Petroleum Report PR4882, 29p.

Contents

Introduction	1
Model Details	1
TQtec Input Parameters	4
Determination of Amount of Erosion	4
Modelling Results for Southern Taranaki Wells	7
Fresne-1.....	7
North Tasman-1.....	9
Survive-1.....	9
Kupe-1.....	11
Confined Track Length Distributions	11
Modelling Results for a Murchison Basin Well	13
Bounty-1.....	15
Model Sensitivity	16
Late Miocene Surface Heat Flow.....	16
Thermal Conductivity.....	17
Burial/Erosion History.....	17
Thermal Modelling of Outcrop Samples	18
Sample 1116-24 (Brunner Coal Measures).....	18
Sample 1116-12 (Scotty Mudstone Member).....	20
Sample 1116-26 (Tutaki Member).....	20
Hydrocarbon Prospectivity in southern Taranaki and Murchison basins	22
Maximum Paleotemperature and Duration of Heating.....	23
Time-Temperature Index and Vitrinite Reflectance.....	25
Timing of Inversion and Maturation.....	26
Acknowledgements	27
References	28

List of Figures

<i>Figure 1.</i> Location map of Southern Taranaki Basin and Murchison Basin hydrocarbon wells/holes. The main faults are labelled. The Wakamarama Anticline is shown as the grey symbol to the north of Fresne-1.	2
<i>Figure 2.</i> Simplified cross-section through Fresne-1 showing the frame of reference for values used in the uplift calculations for southern Taranaki Basin.	5
<i>Figure 3.</i> Observed and predicted apatite track length distributions for modelled samples in Fresne-1, North Tasman-1 and Surville-1.	12
<i>Figure 4.</i> Location map of the Bounty-1 well in Murchison Basin. Map data sourced from the Institute of Geological & Nuclear Sciences QMap project.	14
<i>Figure 5.</i> Cross-section through section line A-A' on Fig. 4. The Bounty-1 well is shown as the blue line. Adapted from Lihou (1993).	15
<i>Figure 6.</i> Map showing sample locations in Murchison Basin. The location of the Bounty-1 well is shown as the black star. The cross-section A-A' is shown in Fig. 7. Map data sourced from the Institute of Geological & Nuclear Sciences QMap project.	19
<i>Figure 7.</i> Cross-section A-A' for Murchison Basin. Approximate locations of samples are shown as black dots. Adapted from Lihou (1993) and Suggate (1984).	19
<i>Figure 8.</i> Measured and modelled apatite track length distributions for sample 1116-24 from the Brunner Coal Measures.	20
<i>Figure 9.</i> Measured and modelled apatite track length distributions for sample 1116-12 from the Scotty Mudstone Member.	21
<i>Figure 10.</i> Measured and modelled apatite track length distributions for sample 1116-26 from the Tutaki Member.	21
<i>Figure 11.</i> Measured track length distributions from this study and from Gibson (1993). Gibson (1993) samples plotted are HR2-22 (Brunner Coal Measures), HR2-37 (Scotty Mudstone) and HR2-17 (Tutaki Member).	22
<i>Figure 12.</i> Measured and modelled track length distributions for sample 1116-24 from the Brunner Coal Measures. Modelled distribution incorporates a cooling period from 35 - 25 Ma, as shown in Table 19.	23
<i>Figure 13.</i> Time-temperature profiles plotted from the FTage output for Fresne-1, North Tasman-1, Surville-1 and Bounty-1 over timescales of a) 80 - 0 Ma, and b) 25 - 0 Ma. The black horizontal line at 80 °C indicates the temperature at the top of the oil window. Figure 13b shows the time spent in the oil generation window given for each well. A second black line at 100 °C shows the starting temperature for significant maturation.	24
<i>Figure 14.</i> Timeline of oil maturation and the formation of key structures in the region of Fresne-1 and Bounty-1 wells. Black stars show the timing of maximum paleotemperature.	26

List of Tables

<i>Table 1.</i> Parameters, constants and units used in the code of TQTec.	3
<i>Table 2.</i> Parameters, constants and units used in the code of FT age.	3
<i>Table 3.</i> Inputs for TQTec.....	4
<i>Table 4.</i> Values used in the calculation of the amounts of uplift and erosion in Fresne-1, North Tasman-1 and Surville-1. Sourced from Jager (2012).	6
<i>Table 5.</i> Burial history for Fresne-1 that gives the best match between observed and predicted AFT ages.	7
<i>Table 6.</i> Observed AFT, predicted AFT and stratigraphic ages for Fresne-1 samples.	8
<i>Table 7.</i> Burial history for North Tasman-1 giving the best match between observed and predicted AFT ages.	10
<i>Table 8.</i> Observed AFT, predicted AFT and stratigraphic age for North Tasman-1 sample 8694-21.	10
<i>Table 9.</i> Burial history for Surville-1 that gives the best match between observed and predicted AFT ages.	11
<i>Table 10.</i> Observed AFT, predicted AFT and stratigraphic age for Surville-1 sample 8694-17.	11
<i>Table 11.</i> Burial history for Bounty-1 that gives the best match between observed and predicted AFT ages.	13
<i>Table 12.</i> Observed AFT, predicted AFT and stratigraphic ages for the Bounty-1 samples.	13
<i>Table 13.</i> Predicted AFT output ages of the four deepest samples in Bounty-1 produced by varying Late Miocene surface heat flow values. Values highlighted in blue have undergone little or no annealing, pink have been partially reset and light green are fully reset ages. The bottom row with values in italics shows the values used in the final model run.	16
<i>Table 14.</i> Predicted AFT ages and the maximum temperature reached by sample HR2-13 with the corresponding Late Miocene surface heat flow values.	16
<i>Table 15.</i> Predicted AFT output ages of the four deepest samples in Bounty-1 produced by varying thermal conductivities. Values highlighted in pink have been partially reset and light green is fully reset ages.	17
<i>Table 16.</i> Burial history for 1116-24 that gives the best match between measured and modelled AFT length distributions.	20
<i>Table 17.</i> Burial history for sample 1116-12 that gives the best match between measured and modelled AFT length distributions.	21
<i>Table 18.</i> Burial history for sample 1116-26 that gives the best match between measured and modelled AFT length distributions.	21
<i>Table 19.</i> Revised burial history for sample 1116-24, including a period of erosion (cooling) between 35 and 25Ma.	23
<i>Table 20.</i> Important stages of oil generation and the corresponding TTI and Ro values (adapted from Waples, 1980).	25
<i>Table 21.</i> TTI and Ro values calculated in FTage for the deepest samples in Fresne-1, North Tasman-1, Surville-1 and Bounty-1.	25

Introduction

Information about surface heat flow is a key parameter in any comprehensive model established to better understand a sedimentary basin's thermal history. In setting up numerical thermal models, a decision needs to be made about the paleo heat flow value to be incorporated in the model. Normally, in the absence of information about paleo heat flow for a basin, the present-day value is commonly used for the duration of the model run. Where there has been substantial erosion of the sedimentary basin succession at some point in the basin history, there will probably have been changes in surface heat flow through time and the value at the point of maximum burial will have the greatest impact on the levels of hydrocarbon maturation. In a comprehensive analysis of the thermal history of multiple Taranaki Basin well successions (Kamp & Green, 1990; Armstrong et al. 1996; Crowhurst et al. 2002), (Fig. 1) the present day surface heat flow value (Funnell et al. 1996) was assumed to apply at the time when the well successions experienced maximum temperatures, prior to up to 100 °C of cooling via up to 3 km of Late Miocene erosion. In this report we address, amongst other objectives, the determination of the surface heat flow in southern Taranaki Basin at the Late Miocene peak burial phase and the start of basin inversion on fault-cored anticlines, which were the exploration targets at the time of drilling.

Such a modelling output requires the burial history of the successions encountered in the holes to be fully understood. We have appealed to the results of seismic reflection mapping of parts of southern Taranaki Basin to determine the amount of Late Miocene and Pliocene erosion of successions in anticlines at Fresne-1, North Tasman-1 and Surville-1, which, historically, have been the output of the application of thermochronology to these well successions (Kamp & Green, 1990; Crowhurst et al. 2002). Having restored the amount of Late Miocene and Pliocene erosion at each of three drill hole sites into the respective burial histories (Fresne-1, North Tasman-1, Surville-1), we then use the thermal modelling code to constrain the surface heat flow value during the Late Miocene

maximum in burial for each of the southern Taranaki Basin sites. In this process we use an extension to the thermal modelling code that predicts fission track parameters (age and track length) and compares them with observed fission track data as a means of validating the model results.

Having established the Late Miocene surface heat flow for southern Taranaki Basin and uncertainty around it, we then use it as input in thermal modelling of the succession encountered in a Murchison Basin well (Bounty-1) to help constrain the amount and timing of erosion of the basin succession during the basin's inversion. We use existing fission track data for Bounty-1 and data for several outcrop samples in Murchison Basin (Gibson, 1993). Based on these results we draw several conclusions about the maturation history of the successions in Taranaki and Murchison basins.

Model Details

The numerical model code used in this study (Furlong & Guzofski, 2000) has been modified in recent years to create burial and exhumation scenarios for given sedimentary columns and to predict apatite fission track (AFT) ages for sample horizons within a sedimentary column that can be compared with data obtained from outcrop or well samples.

There are two components to the thermal modelling code. The first, TQTec, is a finite-difference time-dependant heat diffusion model that, for a given crustal column, solves the conductive heat equation with the burial and exhumation history being the primary input. The output file from TQTec can then be run with readTQTec, which can create temperature, depth, surface heat flow and time histories for the specified depth points input into TQTec. The temperature output file from readTQTec is then opened in FTage, which produces predicted AFT ages for the given depth points, the predicted AFT length distribution, and a temperature history for each depth point time, stepping every 200,000 years. The parameters and constants

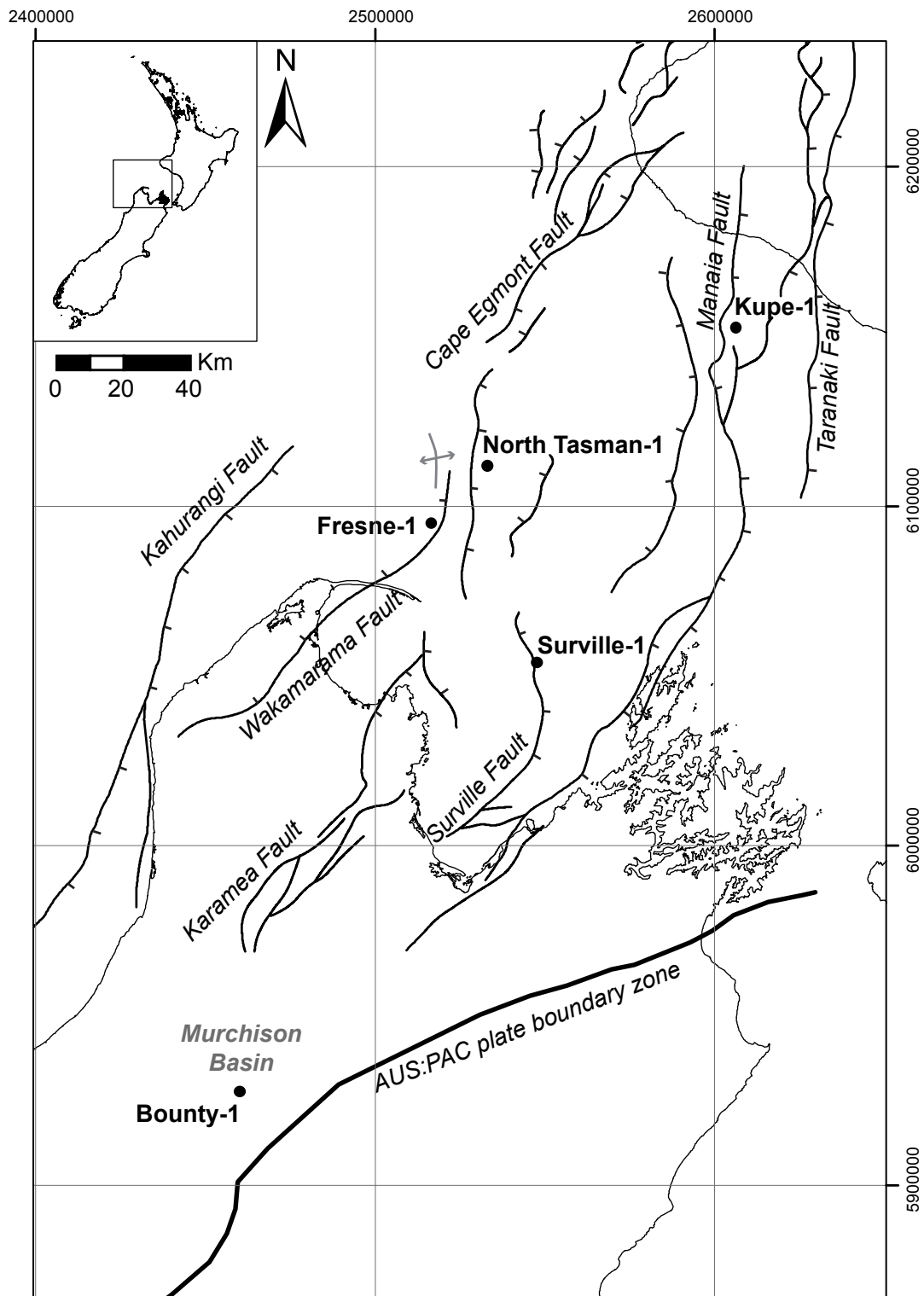


Figure 1. Location map of Southern Taranaki Basin and Murchison Basin hydrocarbon wells/holes. The main faults are labelled. The Wakamarama Anticline is shown as the grey symbol to the north of Fresne-1.

Table 1. Parameters, constants and units used in the code of TQTec.

Parameter	Description	Constant and Units
A	Volumetric heat production	1.0 Wm ⁻³
A ₀	Surface heat production	0.0 Wm ⁻³
D	Depth of heat production	10.0 km
K	Basement thermal conductivity	3.0 Wm ⁻¹ K ⁻¹
K	Thermal diffusivity	32 m ² yr ⁻¹
q	Surface heat flow	* mWm ⁻²
q ₀	Initial surface heat flow	* mWm ⁻²
T	Time	* s
K1	Time step	0.2 m.y.
T	Temperature	* K
T ₀	Surface temperature	288 K (10 °C)
Z	Depth	* km
N	Number of space steps	1200
Ztot	Total depth of model	60 km

* indicates a variable.

Table 2. Parameters, constants and units used in the code of FT age.

Parameter	Description	Constant and Units
A	Empirical rate constant for axial shortening	1.81 μm
h	Planck's constant	1.58E-37 kcal.s
k	Boltzmann's constant	3.2976E-27 kcal.K ⁻¹
l ₀	Initial track length	16.2 (av.) μm
l _{as}	Track length after annealing (uncorrected)	* μm
Q	Activation energy for defect elimination	40.6 kcal.mol ⁻¹
R	Universal gas constant	1.99E-3 kcal.mol ⁻¹ .K ⁻¹
n	Exp. in power-law for initial fission track geometry	0.206
τ	Time interval	0.004 s
T	Temperature	* K
ρ _{st}	Durango apatite age standard	0.893

* indicates a variable.

used for both TQTec and FTage are listed in Tables 1 and 2.

The modelling approach differs to that developed by other authors (e.g. Willett, 1997; Ketcham, 2005) in that it creates 20 fission tracks per time step (as opposed to one single fission track being created per time step) and the track length distribution of the 20 tracks is formulated from the experimental un-annealed track lengths of Green et al. (1986). These track lengths can then be allocated to bins centred on integer length values (in μm) and compared with observed fission track length distributions. Outputs include a model-predicted track length distribution for each depth point, a corresponding fission track retention age and a temperature-time profile with the temperature of each depth point given every 200,000 years from the start to the end of the model. To incorporate the temperature history of an apatite grain into the model, the following equation (Carlson, 1990) is used to calculate annealed lengths:

Equation 1:

$$l_{as} = l_0 - A(k/h)^n \left[\int^t T(\tau) \exp(-Q/RT(\tau)) d\tau \right]^n$$

where l_{as} is the fission track annealed length from an initial length of l_0 created at time τ and $d\tau$ is the duration. $T(\tau)$ is the unit temperature and all other constants are listed in Table 2. The equations utilised in the model to calculate the track length annealing rely on several factors such as apatite composition, anisotropy and the activation energy required for diffusion of displaced atoms back into the crystal lattice (Laslett et al., 1987). Carlson (1990) uses a standard Durango composition on which to base the equations, resulting in the assumption that all samples modelled using FTage have a Durango Apatite composition (fluorapatite, 0.41% wt Cl). This is clearly not the case in reality as experiments carried out by Green et al. (1986) show a significant variation in annealing properties of apatite depending on their chemical composition, particularly their Cl/F ratio. Whilst these differences in composition cannot be incorporated into the model, discrepancies between observed and predicted AFT ages may be contributed in part to differences in composition.

At the end of the model, all tracks are summed and divided by the time step using the following equation (Legg, 2010):

Equation 2:
$$\text{age} = \sum_i l_i / 20 \Delta t_i$$
 where l_i (the annealed and corrected fission tracks) is divided by 20 because 20 tracks are created at each time step.

TQTec Input Parameters

There are a variety of constant and variable inputs required for TQTec, which are summarised in Table 3 and required to be entered during a model run. Several input values remain constant with each model run. The surface temperature is kept at 10 °C as this is a reasonable estimate of the temperature at the seafloor at the present day in southern Taranaki Basin, an assumption being made that this value has not varied significantly in the past. The basement thermal conductivity is taken as 3.0 Wm⁻¹K⁻¹, adopting the value used by Funnell et al. (1996). The surface heat production refers to the influence on heat flow that surface volcanics would have, which in the study areas

Table 3. Inputs for TQTec.

Input	Value Used
Total time for model	Variable (Ma)
Surface temperature	10 °C
Surface heat flow	Variable (mWm ⁻²)
Basement thermal conductivity	3.0 Wm ⁻¹ K ⁻¹
Surface heat production	0.0 Wm ⁻³
10 individual starting depth points	Variable (km)
Number of burials	Variable
Beginning (m.y. after start), duration (m.y.), thickness (km) and thermal conductivity (Wm ⁻¹ K ⁻¹) of each burial period	Variable
Number of erosion periods	Variable
Beginning (m.y. after start), duration (m.y.) and thickness eroded (km) for each erosion period	Variable
Number of thrust events	0

was not an issue during the basin infill history so this value is kept at 0 Wm⁻³.

Certain factors are taken into consideration when entering values for the variable fields. The published stratigraphy for the well or section being modelled is used to create burial intervals with each interval generally equating to the thickness and time span of formations in the established stratigraphy. Similarly, any unconformities present in the section indicate the possible timing of erosion events, however the amount of section removed is generally unknown and must be best estimated in the first run. The range of sample depths in the well is used to determine the starting depth points by creating a succession of starting depths that have the same amount of rock separating them as the samples in the well, to ensure that each depth point finishes the model run at the correct corresponding depth in the well, i.e. if two samples are 500 m apart in a well section, their starting depths must be 500 m apart (sediment compaction is not specifically incorporated in the thermal models). The mean AFT age for each sample in the well is used in determining the total time for the model. If samples have a reset fission track age, the model may begin at the time of deposition of the first stratigraphic unit of interest (deepest well sample). If fission tracks in sample apatite are partially reset or equal to the stratigraphic age, the sample may be modelled individually from the rest of the well section with the start time of the model equal to the depositional age of the unit in which that sample enters the system. If the sample displays a component of inherited age then the start time of the model may be older than the age of deposition of the first stratigraphic unit, to incorporate the effect of inherited age into the final predicted AFT age.

Determination of Amount of Erosion

There are two fundamental unknowns in the TQTec input parameters, which are both required to produce a successful and justifiable match of predicted and observed AFT ages. The first of these is the surface heat flow, for which only present day values are typically known. Attempts

have been made by previous authors to estimate surface heat flow and geothermal gradient in the past (e.g. Funnell et al., 1996; Kamp & Green, 1990; and references therein), however these are derived generally from forward modelling and have not to date been supported by independent geological evidence. Model runs were attempted using the present day surface heat flow for the selected Taranaki wells, however these values ranged from 49 mWm^{-2} to 70 mWm^{-2} (Funnell et al., 1996), giving a wide range of possible values to trial in the Murchison Basin well. Townend (1999) used bottom hole temperature data to estimate the present day surface heat flow at the Bounty-1 well as 73 mWm^{-2} , but as for the southern Taranaki well successions, this does not necessarily represent the surface heat flow in the Late Miocene. The model runs in this study also required a significant amount of trial and error with respect to the amount of section removed during the erosion intervals, despite referring to erosion amount estimates previously published (Knox, 1982; Ellyard & Beattie, 1990; Kamp & Green, 1990; Funnell et al., 1996; Crowhurst et al., 2002, among others). To better constrain the amount of section eroded in the Late Miocene unconformity, this study appealed to the results of recent seismic reflection mapping in southern Taranaki Basin that independently established the amount of erosion at the prominent Late

Miocene unconformity. These values are utilised in the modelling. Using a single value for the amount of section removed by erosion enables a 'paleo' surface heat flow to be determined by trialling different surface heat flow values until a match between the predicted and observed AFT ages is produced. The process to determine the amount of Late Miocene erosion in Fresne-1 relies on the seismic subsurface mapping of several key horizons, detailed in Fig. 2 and described in detail in Jager (2012).

Before considering the amount of erosion, the amount of uplift must first be calculated. To do this the depth of a common reflector must be compared to the depth of that same reflector at a reference point where there has been no late Neogene uplift. In southern Taranaki Basin the age equivalent Tikorangi, Otaoroa and Takaka formations create a laterally continuous thin Oligocene reflector and were consequently mapped as one continuous hybrid horizon. There are several reasons for choosing this horizon:

- (i) The density contrast between the reflector and the formations above and below results in the reflector having a high amplitude that can be easily recognised on seismic sections, even those with relatively low resolution.

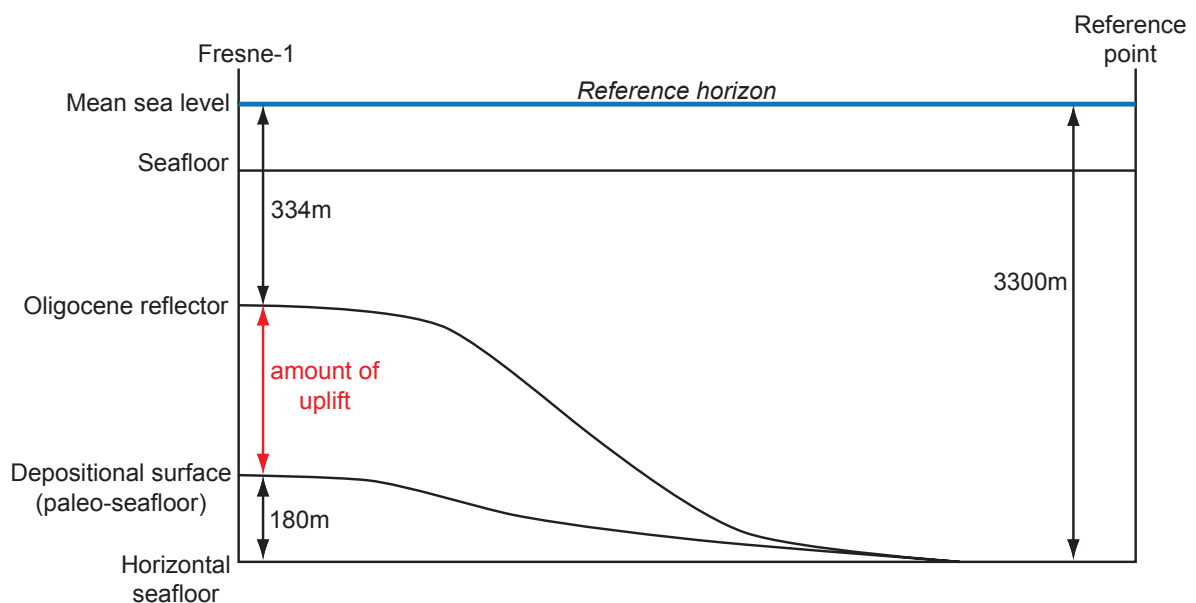


Figure 2. Simplified cross-section through Fresne-1 showing the frame of reference for values used in the uplift calculations for southern Taranaki Basin.

- (ii) The Oligocene sediments are generally less than 100 m thick meaning that they correspond to only one or two seismic reflectors.
- (iii) The reflector is laterally continuous across the whole basin as a result of regional onlap before any late Neogene crustal shortening took place.
- (iv) The Oligocene sediments imaged by the reflector had some variation in bathymetry across the basin, which is reasonably known (Strogen et al. 2011), and is shown as a 180 m difference between the site at Fresne-1 and the reference column on the right hand side in Fig. 2 for which there has been no uplift.
- (v) Throughout the offshore region of southern Taranaki Basin the reflector is completely preserved beneath the Late Miocene unconformity.

In regions where the Oligocene reflector splits into two reflectors, the basal reflector has been mapped for consistency across the basin. The reference column/area is taken as the region in southern Taranaki Basin northwest of the Maari Oil Field and to the east of Pukeko-1 well, where no uplift is considered to have taken place (i.e. the bathymetry has not been affected by crustal shortening as indicated by folding (Jager, 2012)) despite there having been a large amount of Miocene burial. In this reference area, the depth from mean sea level (MSL) to the Oligocene reflector is 3300 m. At Fresne-1, the depth from MSL to the same reflector is only 334 m, which at face value would indicate the amount of uplift to be 2966 m, assuming the Oligocene reflector would have been at the same depth in the reference area had there been no uplift and erosion. The depth to the (Oligocene) paleo-seafloor at well sites must be taken into account however, as seismic mapping shows the paleobathymetry (the surface corresponding to the Oligocene reflector) to have been about 180 m higher in elevation than the same surface at the reference point (this value takes into account some post-Oligocene compaction). More specifically, revised biostratigraphic interpretations from

well completion reports in conjunction with paleogeography maps produced by Strogen et al. (2011) were used to assess the paleogeography as the formations were deposited locally at depths varying from shelf (Takaka Limestone) to upper bathyal (Otaoroa Formation) to mid-lower bathyal (Tikorangi Limestone). Subtracting the paleobathymetry value from the preliminary estimate of uplift, gives a value of 2786 m of net late Neogene uplift.

To calculate the amount of erosion, the thickness of the water column that would first have to be removed before erosion could begin must be subtracted from the total amount of uplift. At Fresne-1 this is estimated to be 100 m based on the inferred paleoenvironment for the area, resulting in a final value of 2686 m for the total amount of Late Miocene erosion. These calculations also assume that the thickness of sediment deposited between the Oligocene and the Late Miocene initiation of inversion was uniform across the basin. Similarly, the effects of decompaction on the sediment thickness are also ignored at inversion structures. This process can be repeated for both North Tasman-1 and Surville-1 (Table 4) to calculate values for the total amount of section removed by Late Miocene - Pliocene erosion processes. The values for Late Miocene erosion can now be entered as a model input to determine the Late Miocene surface heat flow that gives the best fit between the observed and predicted AFT ages for samples in the Taranaki Basin wells.

Table 4. Values used in the calculation of the amounts of uplift and erosion in Fresne-1, North Tasman-1 and Surville-1. Sourced from Jager (2012).

	Fresne-1	North Tasman-1	Surville-1
Depth to Olig. reflector at Reference (m)	3300	3300	3300
Depth to Olig. reflector in well (m)	334	1929	1524
Difference in depth to paleo-seafloor (m)	180	90	150
Amount of uplift (m)	2786	1281	1626
Late Miocene water depth (m)	100	100	0
Amount of erosion (m)	2686	1181	1626

Modelling Results for Southern Taranaki Wells

Fresne-1

Fresne-1 is located in southern Taranaki Basin northwest of Farewell Spit and east of the Wakamarama Fault (Fig. 1). It penetrates over 3 km of Cretaceous to Recent sediment on the hinge of the Wakamarama Anticline, an inversion structure originating from Late Miocene reverse movement on pre-existing normal faults. Previous thermal modelling of the Fresne-1 succession has been undertaken by Kamp & Green (1990) and Crowhurst et al. (2002) to constrain the amount of late Neogene uplift and erosion. Kamp & Green (1990) suggested that three km of erosion occurred between 12 and 8 Ma, based on a geothermal gradient equal to that of the present day at 28 °C/km (equating to a surface heat flow of 64 mWm⁻²). Crowhurst et al. (2002) used the same geothermal gradient to calculate a value for the amount of section removed by erosion, giving a preferred value of 2675 m (the midpoint between their upper and lower estimates of 2800 m and 2550 m). As seen in Table 4, the value for erosion calculated from seismic mapping matches quite closely the Crowhurst et al. (2002) value, so a value of 2700 m will be used in the modelling (the maximum resolution of the model is 50 m).

The present day surface heat flow at Fresne-1 is one of the highest in Taranaki Basin at 70 ± 12 mWm⁻² (Funnell et al., 1996). The first model runs use this value and progressively refine it until there is a match between the observed and predicted fission track ages. There are eight sample points with AFT ages (Crowhurst et al. 2002) in Fresne-1. The three deepest samples (8694-14, 13 and 12) range in depth from 2480 to 1889 m and all have overprinted AFT ages; that is,

the sample apatite were situated below the partial annealing zone before Late Miocene exhumation started, during which they began to accumulate tracks. Samples 8694-11, -10 and -9 all have partially annealed ages, which are younger than the respective stratigraphic ages consistent with residence in the partial annealing zone prior to the start of cooling through erosion. The two shallowest samples (8694-8 and -7) display AFT ages older than their stratigraphic ages indicating that they entered the basin with a component of inherited age.

The fission track parameters for the samples are modelled as for a continuous sedimentary section that moves vertically with each sample entering the system at its stratigraphic age. The burial history is constructed using the well stratigraphy as reported in King & Thrasher (1996), completed by the erosion data shown in Table 4. The thermal conductivities for each burial layer are derived from Funnell et al. (1996) or are a best estimate based on the lithology of the formation. The final burial history that produces the best fit of the observed and predicted AFT ages and track lengths has the inputs listed in Table 5.

Table 5. Burial history for Fresne-1 that gives the best match between observed and predicted AFT ages.

Burial Start Time (Ma)	Burial End Time (Ma)	Thickness Deposited (m)	Thermal Conductivity (Wm ⁻¹ K ⁻¹)	Equivalent Formation/Member
78	77	150	3.36	North Cape
77	69	700	3.36	North Cape
69	65	200	3.26	Puoponga
65	52	800	3.10	Farewell
29	27.5	50	3.00	Abel Head
27.5	25	50	3.00	Takaka Limestone
25	17.5	100	2.50	Kaipuke Siltstone
17.5	14.5	2000	2.80	Manganui
14.5	10	1050	2.80	Manganui
2	0	100	2.80	Recent sediments
Erosion Start Time (Ma)	Erosion End Time (Ma)	Thickness Eroded (m)		
52	29	0		
8	6	500		
6	4	1200		
4	2	1500		

There is a period (10 - 8 Ma) for the Fresne-1 area during which there is no deposition or erosion, which is incorporated into the burial history to represent uplift with no erosion, i.e. the removal of water depth before the seafloor and underlying sediments were subjected to erosion. The 0 m of erosion between 47 and 29 Ma is a best estimate as there are no values published for the amount of section removed during the Eocene – Oligocene, if at all. The 2700 m of section removed during the Late Miocene inversion is split into three intervals in this burial history to simulate the slow erosion rates shortly after emergence when the terrain was at low elevations, followed by more rapid erosion as the topography grew over time. This subdivision into three erosion intervals also allows for better modelling of the observed and predicted AFT ages. Initial model runs that had just one interval of Late Miocene - Pleistocene erosion (8 - 2 Ma) did not allow the very deepest samples to remain at elevated temperatures long enough to fully anneal and reset the fission track parameters, so a slower erosion rate was introduced at the start to ensure the deeper sample could remain in the partial annealing zone for longer, allowing more tracks to be shortened. Table 6 shows the match between the observed AFT ages published by Crowhurst et al. (2002) with the corresponding ages predicted by FTage produced from the burial history in this study (Table 5).

To produce the best fitting ages, a Late Miocene surface heat flow of 79 mWm^{-2} is required as an input value corresponding to the time of maximum burial. This compares with the

present day value adopted by Funnell et al. (1996) of $70 \pm 12 \text{ mWm}^{-2}$. An error of 6 mWm^{-2} can be placed on the value of 79 mWm^{-2} . This value was determined by the fact that heat flow values less than 73 mWm^{-2} or higher than 85 mWm^{-2} produce modelled AFT ages that do not match any of the measured AFT ages. As soon as the heat flow is altered to be within 6 mWm^{-2} of the 79 mWm^{-2} value, there is at least one match between the modelled and measured AFT ages to within the error associated with each measured AFT age.

In terms of maximum paleotemperature, the temperature reached by the deepest sample prior to the start of cooling is predicted to be $118 \text{ }^\circ\text{C}$, which is lower than previous estimates of $139 \text{ }^\circ\text{C}$ based on vitrinite reflectance data (Crowhurst et al., 2002). Maximum paleotemperature for all of the remaining samples are higher than those modelled here (Armstrong et al., 1996; Crowhurst et al., 2002; Kamp & Green, 1990) as the temperatures previously suggested for the shallower apatite samples would result in overprinting and considerable annealing of their fission tracks, consequently producing much younger mean ages (all previous paleotemperature estimates for the shallowest sample are equal to or in excess of $100 \text{ }^\circ\text{C}$). Constraining the maximum paleotemperature for the horizons in the well is not only important when considering the generation and annealing of fission tracks, but also in the assessment of the potential for hydrocarbon prospectivity in the region, which is discussed below.

Table 6. Observed AFT, predicted AFT and stratigraphic ages for Fresne-1 samples.

Sample 8694-	Present depth in well (m)	Observed AFT age (Ma)	Predicted AFT age (Ma)	Stratigraphic age (Ma)	Maximum Temperature ($^\circ\text{C}$)
7	430	77.0 ± 3.5	35.50	53	81
8	705	64.9 ± 4.8	46.05	59	86
9	1058	28.6 ± 4.5	35.82	66	93
10	1330	22.0 ± 4.6	25.76	68	97
11	1635	13.3 ± 2.9	10.31	70	104
12	1900	5.5 ± 0.9	6.39	72	108
13	2110	4.9 ± 0.7	4.87	75	114
14	2465	8.5 ± 2.4	4.30	77	118

North Tasman-1

North Tasman-1 is located to the northeast of Fresne-1 (Fig. 1) and passes through over 2.5 km of Cretaceous - Recent sediment before reaching basement granite. This well differs from Fresne-1 in that it contains a very thick Miocene succession with around 1700 m of section lying between the Eocene - Oligocene unconformity and the Late Miocene unconformity. Thermal modelling undertaken by Kamp & Green (1990) suggests that the three deepest of the four samples within North Tasman-1 were slightly hotter in the past but no significant annealing of track lengths has taken place (the deepest sample is in fact taken from the basement granite and so will not be included in the thermal modelling discussed here). The two shallower samples, 8694-19 and -20, both have AFT ages that are much older than the stratigraphic age of the host sediment, indicating a significant component of inherited age. The deepest sedimentary sample, 8694-21, has an AFT age equal to the stratigraphic age, but given that there are a number of tracks shorter than 10 μm , suggests that some annealing has taken place after deposition (Kamp & Green, 1990). The modelling will focus on this one sample as there is no way of knowing the inherited age or track length distribution of the apatite in the two shallower samples at the point the apatite in those samples were deposited. As the fission tracks in the apatite in the sample of interest are not fully annealed, it is only possible to model a maximum surface heat flow, which, if exceeded, results in too much annealing and a reduction in the AFT age below the observed value. In terms of maximum paleotemperature experienced, Kamp & Green (1990) suggested that temperatures could not have exceeded 120 °C, otherwise there would have been a more significant reduction in track lengths. This limits the amount of Late Miocene erosion that has taken place as there has only been a reduction in temperature of approximately 25 °C between maximum burial and the present day, giving erosion estimates of 1350 m (Knox, 1982) and 1000 m (Kamp & Green, 1990). As with Fresne-1, the amount of Late Miocene erosion that will be used as a model input is calculated from seismic mapping and is listed in Table 4. The value of 1181 m (1200 to the nearest 50 m) is between the erosion estimates

given by Knox (1982) and Kamp & Green (1990) and is adopted in the modelling. The thickness removed during the Eocene - Oligocene period of quiescence is also unknown so is estimated at 50 m, with erosion occurring between 35 and 29 Ma. A period of non-deposition or erosion is also incorporated before each L. Miocene erosion period to represent the removal of water depth during initial uplift (from 37 - 35 Ma and 10 - 8 Ma). Table 7 shows the reconstructed burial history for North Tasman-1 that produced the best fit of the observed and predicted AFT age for sample 8694-21, for which the results are given in Table 8.

The maximum surface heat flow used with this burial history is 82 mWm^{-2} . Any higher value and too much annealing takes place and the predicted AFT age is reduced below that observed for the sample. This is significantly higher than the present day value given by Funnell et al. (1996) of $64 \pm 9 \text{ mWm}^{-2}$, but given that it is a maximum surface heat flow, the paleo-surface heat flow could certainly be within the range of the present day value and could certainly have been higher in the past as shown to be the case at the Fresne-1. A surface heat flow of 82 mWm^{-2} results in sample 8694-21 reaching a maximum temperature of 79 °C, which is not hot enough to cause any significant annealing but would result in the appearance of some shorter tracks, as observed in the track length distribution (Kamp & Green, 1990). This value is significantly less than those published by other authors, but as mentioned above, if the temperature had been higher there would be a noticeable reduction in the AFT age.

Surville-1

Surville-1 is located to the southeast of North Tasman-1 and Fresne-1 on the northern section of the Surville Fault (Fig. 1). Basement granite lies below 2 km of Eocene to Recent sedimentary section. The modelling of fission track data for Surville-1 must be treated a little differently to data for Fresne-1 and North Tasman-1 because the hole does not penetrate Cretaceous sediments and the Neogene erosion at Surville-1 started before uplift and loss of water depth started at Fresne-1 and North Tasman-1 (Table

Table 7. Burial history for North Tasman-1 giving the best match between observed and predicted AFT ages.

Burial Start Time (Ma)	Burial End Time (Ma)	Thickness Deposited (m)	Thermal Conductivity ($\text{Wm}^{-1}\text{K}^{-1}$)	Equivalent Formation/Member
77	65	400	3.36	North Cape
65	37	300	3.24	Farewell
29	22	50	3.00	Abel Head
22	19	100	2.50	Kaipuke Siltstone
19	16	150	2.80	Manganui/Tarakohe
16	15	450	3.33	Moki
15	14	500	2.80	Manganui
14	13	50	3.09	Mt. Messenger
13	10	1450	2.80	Manganui
2	0	200	2.80	Recent sediments

Erosion Start Time (Ma)	Erosion End Time (Ma)	Thickness Eroded (m)
35	29	50
8	2	1200

Table 8. Observed AFT, predicted AFT and stratigraphic age for North Tasman-1 sample 8694-21.

Sample	Present depth in well (m)	Observed AFT age (Ma)	Predicted AFT age (Ma)	Stratigraphic age (Ma)	Maximum Temperature ($^{\circ}\text{C}$)
8694-21	2275	67.8 ± 5.3	64.20	68	79

4). As for North Tasman-1, Surville-1 contains four AFT samples, the deepest of which is granitoid basement and will not be included in the modelling. The three shallower sedimentary samples all have very similar AFT ages, which are all significantly older than the stratigraphic age, indicating that little if any annealing has taken place. Inspection of the track lengths by Kamp & Green (1990) however would suggest that some degree of annealing has taken place, as the majority of track lengths in each well sample are generally shorter than expected with mean track lengths between 10 and 12 μm . They placed an estimate on the amount of uplift and erosion of 2 km, based on the assumption that paleotemperatures were approximately 40 $^{\circ}\text{C}$ hotter than the present day (given the proportion of tracks with reduced lengths). Based on detailed seismic mapping the amount of Late Miocene erosion adopted is 1626 m (Table 4), resulting in

a value of 1650 m being used in the modelling (rounding to the nearest 50 m). A period of non deposition or erosion is included in this model but is reduced to a period of 1 m.y., based on the assumption that uplift began at 10 Ma as for Fresne-1 and North Tasman-1 but that the Surville-1 sediments were being actively eroded by 9 Ma instead of 8 Ma. In contrast to North Tasman-1, only a minimum surface heat flow value can be obtained in the modelling of Surville-1 fission track data. This is the lowest heat flow required to start annealing if an apatite entered the sedimentary system with an inherited age equal to the observed AFT age. Any lower than this value and no annealing would take place resulting in no shortening of track lengths. Table 9 shows the model input parameters that produced the fit between the observed and predicted AFT ages (Table 10), with the minimum surface heat flow required to start annealing being 73 mWm^{-2} .

The burial history for Surville-1 required the model run to begin at 79 Ma with the sample apatite residing near the surface until the start of burial to simulate the inherited age. Using a surface heat flow value lower than 73 mWm^{-2} results in no annealing taking place and the predicted AFT age stays at 79 Ma equal to the observed AFT age. Despite this value only being a minimum, it does fit well with the regional trend and the actual paleo surface heat flow could well have been in the region of the maximum burial values estimated for Fresne-1 and North Tasman-1. It would be difficult to place a maximum value on the surface heat flow as there is no way of knowing the inherited age or track length distribution with which the apatite entered the basin. In terms of maximum paleotemperature, the highest temperature reached by sample 8694-17 with a surface heat flow of 73 mWm^{-2} would be 74 $^{\circ}\text{C}$,

Table 9. Burial history for Surville-1 that gives the best match between observed and predicted AFT ages.

Burial Start Time (Ma)	Burial End Time (Ma)	Thickness Deposited (m)	Thermal Conductivity ($\text{Wm}^{-1}\text{K}^{-1}$)	Equivalent Formation/Member
30	26	200	3.13	Brunner
26	24	100	2.9	Abel Head
24	23	50	2.9	Takaka
23	22	100	2.7	Taimana
22	19	300	2.4	Kaipuke
19	17	600	2.8	Manganui
17	10	1950	3.33	Mokau
2	0	100	2.8	Recent sediments

Erosion Start Time (Ma)	Erosion End Time (Ma)	Thickness Eroded (m)
9	7	1650

Table 10. Observed AFT, predicted AFT and stratigraphic age for Surville-1 sample 8694-17.

Sample	Present depth in well (m)	Observed AFT age (Ma)	Predicted AFT age (Ma)	Stratigraphic age (Ma)	Maximum Temperature ($^{\circ}\text{C}$)
8694-17	1745	78.9 ± 3.8	73.21	30	74

which is considerably lower than the 90 - 100 $^{\circ}\text{C}$ estimated by Kamp & Green (1990). It must be remembered, however, that this model considers a minimum surface heat flow and therefore 74 $^{\circ}\text{C}$ would be a minimum paleotemperature for the deepest sedimentary sample.

Kupe-1

Kupe-1 is located to the north of the three previous wells just to the east of the Manaia Fault (Fig. 1) and intersects over 3.5 km of Paleocene to Recent section. The observed AFT ages from the six samples within Kupe-1, however, do not allow them to be modelled to estimate paleotemperature. All of the observed AFT ages are significantly older than their stratigraphic ages (Kamp & Green, 1990) and increase in age with increasing depth in the well (the opposite pattern to Fresne-1). This indicates that there has not been enough burial heating in the past or residence at elevated temperatures to heat the samples

enough to anneal the track length distributions beyond the level appropriate to present day temperatures. There has also been substantial burial during the Pliocene resulting in the sample points below the Late Miocene unconformity currently residing at similar levels to those prior to the start of Late Miocene erosion (despite minor erosional unconformities at the base of the Opoitian Matemateaonga Formation), unlike the previous three wells in which the samples were buried much deeper in the past. This means that the Kupe-1 samples are presently at their maximum paleotemperature, which does not allow effective modelling of the thermal history for the well section, but does provide information about the potential for hydrocarbon exploitation in the well, as discussed below.

Confined Track Length Distributions

One of the major benefits of this modelling process is that multiple samples can be modelled as one continuous sedimentary column. This differs from most other models that use fission track data, as these tend to only allow modelling of one sample at a time. By creating a burial and exhumation history that simultaneously models confined track length data for several samples, better constraints can be placed on the thermal history of the sedimentary succession than if only one sample is modelled. To test the burial histories defined in Section 5, confined track length distributions for samples from Fresne-1, North Tasman-1 and Surville-1 can be modelled and compared with the measured horizontally confined track lengths reported in Kamp & Green (1990).

FT age creates 20 fission tracks per time step and the track length distribution of the 20

tracks is formulated from the experimental un-annealed track lengths of Green et al. (1986) and the thermal history using Equation 1 (Carlson, 1990) (see page 3). For each southern Taranaki Basin well (excluding Kupe-1) a comparison between the observed and predicted track length distributions can be plotted, as shown in Fig. 3.

The two deeper samples in Fresne-1 (8694-13

and -12) show a good correlation between the observed and predicted track length distributions, particularly for 8694-13 in which both peaks are at 14 μm . Sample 8694-12 does have a minor peak in the predicted length distribution at 8 μm , which is not mirrored in the observed histogram. This may be due to the influence of inherited tracks with some apatite entering the system with long tracks (in excess of 15 μm), which are then

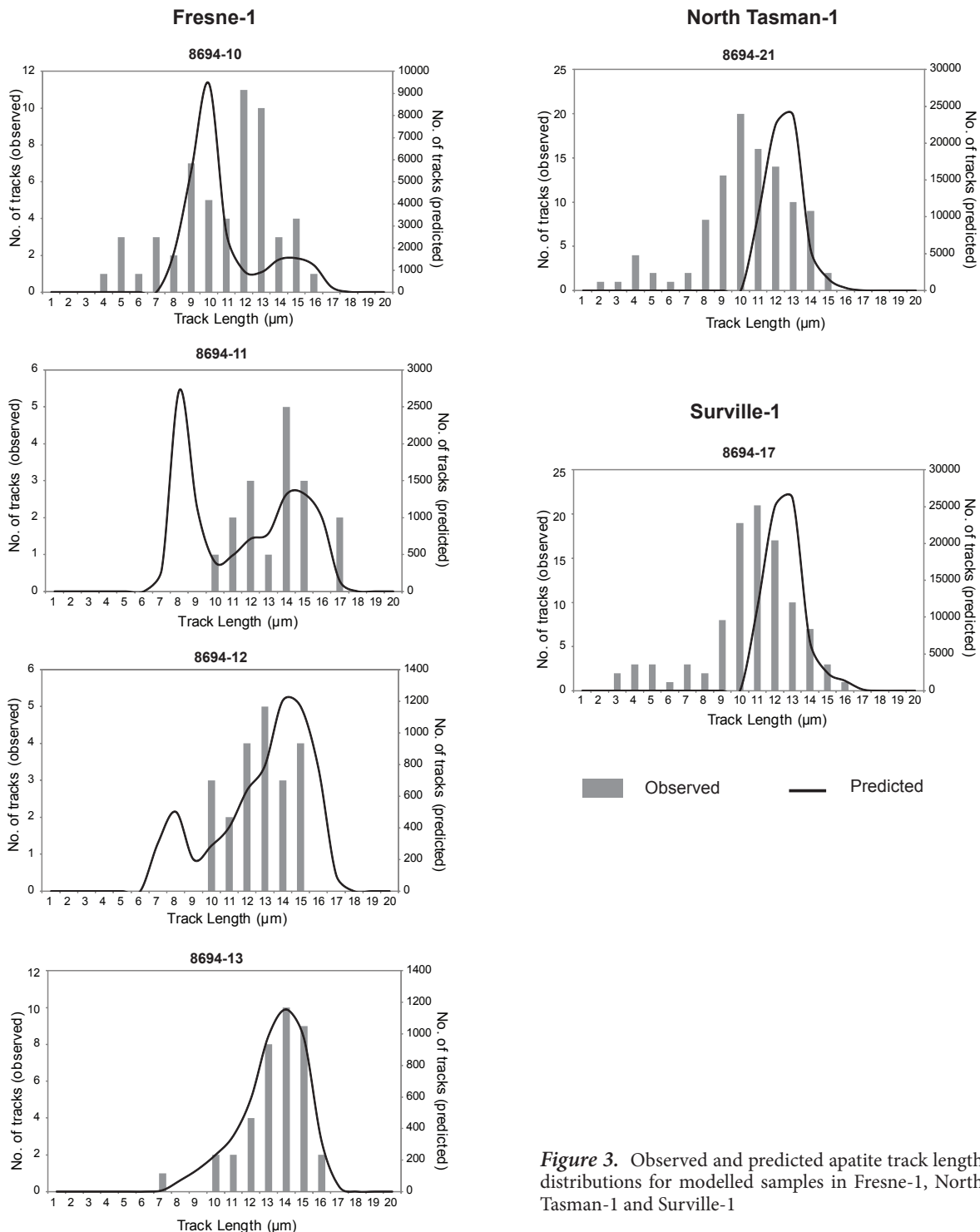


Figure 3. Observed and predicted apatite track length distributions for modelled samples in Fresne-1, North Tasman-1 and Surville-1

annealed enough to shorten by several microns. This would place them in the 10 - 14 μm range in which the majority of the observed tracks fall, rather than in the 7 - 10 μm range in which they would be situated if they entered the system with no inherited tracks. The two shallower samples, 8694-11 and -10, display a mismatch between the observed and predicted peaks of track length frequency. In both cases the predicted track length peak is at a shorter track length than the observed histogram peak. As with the previous sample, this is most likely due to the effect of inherited track lengths that have annealed into the 10 - 14 μm range but would in fact be much shorter had those tracks only begun to form when the apatite entered the burial system. Sample 8694-10 also displays a much greater spread of observed track lengths than both the predicted distribution and the three deeper samples. Those shorter tracks may be present because the sample did not get hot enough to fully anneal any short tracks that were inherited. This is the most likely explanation for the differences between the observed and predicted peaks for the modelled samples in both North Tasman-1 and Surville-1. Neither sample (8694-17 and -21) reaches a temperature high enough (neither exceeds 80 $^{\circ}\text{C}$) to completely anneal inherited tracks, resulting in those tracks simply becoming shortened rather than being removed altogether as they would be if the sample had been buried to a deeper level.

Modelling Results for a Murchison Basin Well

The values obtained for Late Miocene surface heat flow from modelling of selected southern Taranaki Basin wells can now be utilised in the modelling of AFT data for samples from an onshore well in the Murchison

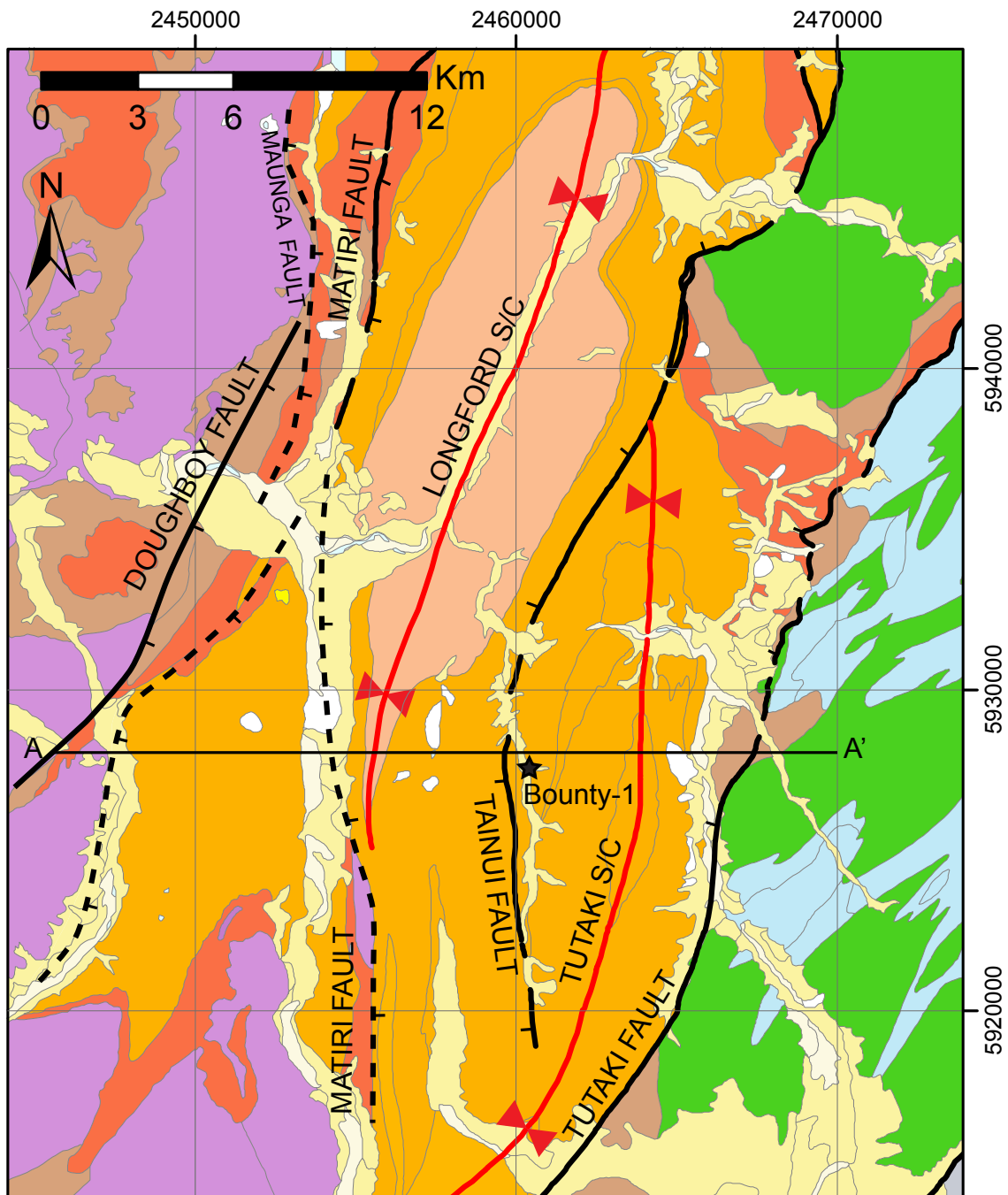
Basin (Bounty-1) (Table 12). This will place constraints on the burial and exhumation history of the basin in the vicinity of the Bounty-1 well in the central part of the basin. Figure 4 shows the location of the Bounty-1 well and a corresponding cross-section along section line A-A' is shown in Fig. 5. From North Tasman-1 and Surville-1 a minimum and maximum can be placed on the regional Late Miocene paleo-surface heat flow value with the value for Fresne-1 lying within that range. The range of surface heat flow values ranges from 73 to 82 mWm^{-2} with an average of 77 mWm^{-2} , which is used in the first instance in modelling the AFT data for the Murchison Basin well. Bounty-1 is located in the southeast part of Murchison Basin, just to the east of Tainui Fault, and was drilled in the late 1960s to test the hydrocarbon potential of the Eocene and Oligocene succession.

Table 11. Burial history for Bounty-1 that gives the best match between observed and predicted AFT ages.

Burial Start Time (Ma)	Burial End Time (Ma)	Thickness Deposited (m)	Thermal Conductivity ($\text{Wm}^{-1}\text{K}^{-1}$)	Equivalent Formation/Member
40	27	800	2.5	Brunner Coal - Scotty
27	24	400	2.5	Scotty/Doughboy
24	23	200	2.5	Scotty/Trig M
23	19	1800	3.4	Tutaki
19	14	200	3.2	Crowe/Valley Creek
14	9	2500	3.2	Longford
9	8	500	3.2	Rappahannock
Erosion Start Time (Ma)	Erosion End Time (Ma)	Thickness Eroded (m)		
8	4	800		
4	0	1750		

Table 12. Observed AFT, predicted AFT and stratigraphic ages for the Bounty-1 samples.

Sample	Present depth in well (m)	Observed AFT age (Ma)	Predicted AFT age (Ma)	Stratigraphic age (Ma)	Maximum Temperature ($^{\circ}\text{C}$)
HR2-91	2100	10.6 \pm 2.7	11.49	22	92
HR2-92	2403	10.5 \pm 3.5	8.12	23	97
HR2-11	2795	3.1 \pm 1.2	3.56	25	107
HR2-13	3103	1.2 \pm 0.7	2.25	28	115



Murchison Geological Map - Legend



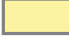






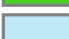


- | | | | |
|---|------------------------|---|---------------------------------|
|  | Sands |  | Fault (tick on downthrown side) |
|  | Sands and Gravels |  | Syncline |
|  | Longford Formation |  | Well Location |
|  | Mangles Formation | | |
|  | Matiri Formation | | |
|  | Maruia Formation | | |
|  | Separation Point Suite | | |
|  | Rotoroa Complex | | |
|  | Karamea Suite | | |

Figure 4. Location map of the Bounty-1 well in Murchison Basin. Map data sourced from the Institute of Geological & Nuclear Sciences QMap project.

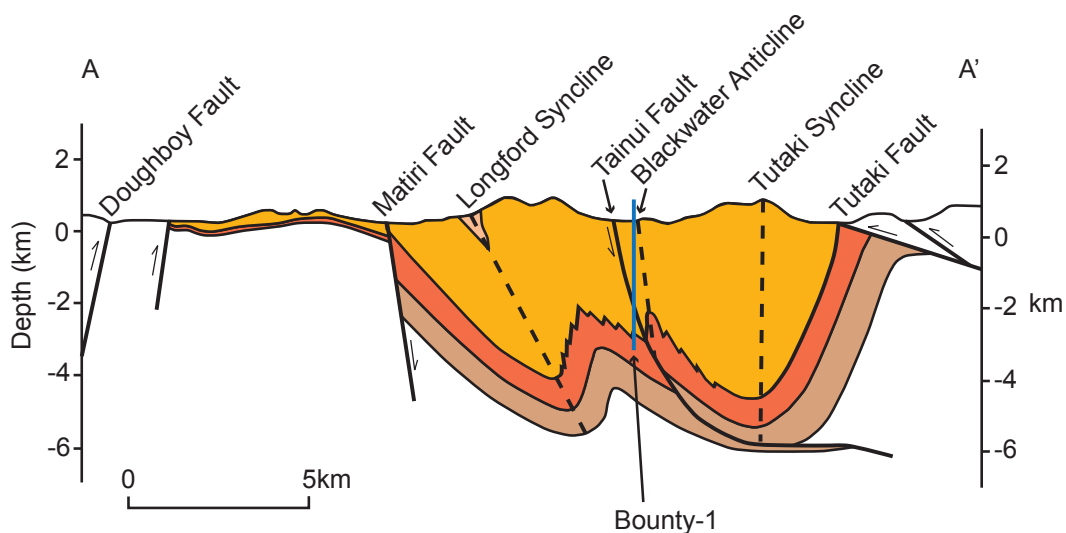


Figure 5. Cross-section through section line A-A' on Fig. 4. The Bounty-1 well is shown as the blue line. Adapted from Lihou (1993).

Bounty-1

Bounty-1 is the southernmost well located in the Blackwater Anticline in the Tainui Fault Zone (as defined by Suggate (1984)). It penetrates over 3 km of Oligocene to Middle Miocene section. There has been erosion of a substantial part of the basin fill, chiefly the upper part, since the Late Miocene. The amount of section removed is poorly constrained but considered to be of similar magnitude to the section eroded in the southern Taranaki Basin wells (Gibson, 1993). The estimates of the thickness eroded are essentially based on reconstruction of the total rock column from outcrop of the youngest stratigraphic units that still exist within the basin, particularly the Late Miocene Longford Formation. From outcrop, the Longford Formation has an approximate thickness of 2.7 km (Suggate, 1984), which could provide a starting point for the amount of erosion at Bounty-1, given that the shallowest units in the hole belong to the Early Miocene Tutaki Member of the Mangles Formation. An assumption is also made that the Rappahannock Group, which crops out in the Maruia Basin, formerly accumulated above the Longford Formation in Murchison Basin. Eight samples were obtained from Bounty-1 and AFT data were collected by Gibson (1993). The deepest four samples have either reset or partially annealed fission track parameters. The four shallower samples have a component of inherited age and the fission track ages are older than the corresponding stratigraphic ages.

The burial history that provided the best match between the observed and predicted AFT ages is shown in Table 11, based on an average surface heat flow of 77 mWm^{-2} at the peak of burial. This burial history requires 2550 m of erosion to have occurred from 8 Ma to the present, which is certainly comparable to the values for Southern Taranaki wells, given that the Murchison Basin is now subaerial and continuing to be uplifted and eroded during the Pliocene and Pleistocene as a result of shortening across the Alpine Fault. As the upper Longford Formation and the younger Rappahannock Formation both accumulated in fluvial environments, Late Miocene erosion would not have been preceded by uplift and removal of water depth. The maximum paleotemperature experienced by the deepest sample is $115 \text{ }^\circ\text{C}$, with the three shallower samples being heated to temperatures of $107 \text{ }^\circ\text{C}$, $97 \text{ }^\circ\text{C}$ and $92 \text{ }^\circ\text{C}$, respectively. An error of 5 mWm^{-2} can be placed on the surface heat flow value of 77 mWm^{-2} to encompass the maximum and minimum surface heat flow determined in the modelling of the North Tasman-1 and Surville-1 wells (maximum of 82 mWm^{-2} and minimum of 73 mWm^{-2}). When modelling the AFT ages with these maximum and minimum surface heat flow values, the amount of erosion must be altered to match the modelled and measured AFT ages. Therefore the amount of erosion at the Bounty-1 well could potentially range from 2250 m (surface heat flow of 82 mWm^{-2}) to 2700 m (surface heat flow of 72 mWm^{-2}).

Model Sensitivity

TQTEC requires a variety of input parameters all of which will have an influence on the predicted AFT age output. It is therefore necessary to assess the effect of altering these parameters on the output ages to determine the sensitivity of the predicted fission track age to various input parameters. The three parameters assessed are the Late Miocene surface heat flow, the thermal conductivity of the sediments and the burial/erosion history.

Late Miocene Surface Heat Flow

Late Miocene surface heat flow, defining the geothermal gradient, has a direct effect on the maximum temperature reached by buried sediments. This consequently affects the predicted AFT age, as the samples must reach a certain temperature before thermal annealing can take place. To test the sensitivity of the AFT age to changes in surface heat flow, the burial history for Bounty-1 was run with a range of different Late Miocene surface heat flow values from 58 to 82 mWm⁻². These values correspond to the present day value assigned to Fresne-1 (Funnell et al., 1996) of 70 ± 12 mWm⁻² and cover the broad range of Late Miocene surface heat flow values estimated for southern Taranaki Basin wells. The AFT ages produced by each model run are shown in Table 13.

The AFT age from the thermal modelling varies significantly for each sample depending on the Late Miocene surface heat value entered as

Table 13. Predicted AFT output ages of the four deepest samples in Bounty-1 produced by varying Late Miocene surface heat flow values. Values highlighted in blue have undergone little or no annealing, pink have been partially reset and light green are fully reset ages. The bottom row with values in italics shows the values used in the final model run

Heat Flow (mWm ⁻²)	HR2-13 (Ma)	HR2-11 (Ma)	HR2-92 (Ma)	HR2-91 (Ma)
58	17.21	20.57	21.72	22.32
64	8.64	15.42	18.86	20.99
70	3.83	8.02	14.53	18.19
76	2.40	3.93	8.48	14.04
82	1.60	2.67	4.93	8.21
77	2.25	3.56	8.12	11.49

a model input. In many cases an increase of 6 mWm⁻² in the paleo heat flow will cause a sample undergoing no annealing to be either partially or fully reset. Surface heat flow can only be entered as an integer value in TQTEC, so the next step is to evaluate the effect on the AFT age of increasing the heat flow by 1 mWm⁻². The model was run with heat flow values ranging from 58 to 70 mWm⁻² and the results for the deepest sample, HR2-13 are shown in Table 14.

Table 14. Predicted AFT ages and the maximum temperature reached by sample HR2-13 with the corresponding Late Miocene surface heat flow values.

Heat Flow (mWm ⁻²)	Age (Ma)	Maximum Temperature (°C)
58	17.21	87.7
59	16.96	89.1
60	13.03	90.5
61	12.58	91.9
62	12.26	93.4
63	9.13	94.8
64	8.64	96.2
65	8.31	97.6
66	6.08	99.1
67	5.69	100.5
68	5.39	101.9
69	4.12	103.3
70	3.83	104.8

Increasing the heat flow by 1 mWm⁻² results in an incremental increase in the maximum temperature of 1.4 °C. The AFT age however does not always increase by a constant amount with increases ranging from 0.25 m.y. to 3.93 m.y. This is particularly noticeable at the lower surface heat flow values with an almost 4 m.y. decrease in AFT age between 59 and 60 mWm⁻². This is probably a result of the sample reaching a predefined temperature within the TQTEC code at which a greater degree of annealing can take place; that is, the point at which the sample enters the partial annealing zone. Entering the partial annealing zone would consequently result in the sample having a much lower predicted AFT age as many more tracks will be shortened and annealed.

A change in maximum temperature will also affect the hydrocarbon maturation of the source rocks. The Bounty-1 well was drilled to test the Matiri

and Maruia formations for oil and gas maturation but never reached the Maruia Formation source rocks. The maximum temperatures of the Maruia Formation units would follow the same pattern as that of sample HR2-13 shown in Table 14, but would be between approximately 10 and 20 °C hotter. This places the rocks at the higher end of the oil producing window if significant oil production from kerogen takes place at temperatures between 80 and 150 °C (Bjørlykke, 2010). Most of the maturation process takes place between temperatures of 100 to 150 °C so a higher heat flow would produce a more mature oil assuming the rocks have resided at the maximum temperature for a long enough period.

Thermal Conductivity

The second parameter to have an effect on predicted AFT ages is the thermal conductivity of the sediment layers put into the burial history. To assess the influence of changing the thermal conductivity, the value will be altered for the first four burial periods (from 40 - 19 Ma) in the Bounty-1 burial history. These four burials contain the four deepest well samples in Bounty-1. That is, they represent the geological formations from which the samples were obtained, and for which each was assigned an original thermal conductivity value based on the overall lithology of the formation (2.5 Wm⁻¹K⁻¹ for burial intervals 1 - 3, and 3.4 Wm⁻¹K⁻¹ for burial interval 4). In the sensitivity tests all four burial intervals were given the same value for thermal conductivity, ranging from 1.5 - 4.0 Wm⁻¹K⁻¹, the results of which are given in Table 15.

Table 15. Predicted AFT output ages of the four deepest samples in Bounty-1 produced by varying thermal conductivities. Values highlighted in pink have been partially reset and light green is fully reset ages.

Thermal Conductivity of Burials 1-4 (Wm ⁻¹ K ⁻¹)	HR2-13 (Ma)	HR2-11 (Ma)	HR2-92 (Ma)	HR2-91 (Ma)
1.5	0.00	0.07	0.60	1.79
2.0	0.23	0.71	2.05	3.63
2.5	1.01	1.87	3.51	6.10
3.0	2.20	3.25	6.01	10.76
3.5	3.22	4.59	8.53	14.04
4.5	4.42	8.02	11.27	14.53

For low thermal conductivity values, AFT ages are very young because the sediments will retain heat for much longer (despite taking more time to heat up in the first instance), resulting in a greater degree of annealing. As thermal conductivities increase, heat is more easily lost from the sediments causing a decrease in temperature and a lesser amount of annealing. Similarly, if a formation with low thermal conductivity overlies a formation with a higher value, the overlying sediments will create a blanketing effect allowing heat to be trapped in the underlying unit(s). The reverse situation has the opposite effect with overlying layers allowing heat to be conducted away from the deeper formations that have lower thermal conductivities. This is applicable to the model input for Bounty-1, which assigns values of 2.5 Wm⁻¹K⁻¹ to burial intervals 1, 2 and 3 and a higher value of 3.4 Wm⁻¹K⁻¹ to burial interval 4. This allows the first three formations to have a thermal conductivity that best fits the lithology (predominantly mudstone and siltstone of the Scotty Mudstone and Trig M Member), but stops the fission tracks in the apatite from annealing too much by having a much higher thermal conductivity for the overlying Tutaki Member sandstone, allowing heat to conduct away from the lower units.

Burial/Erosion History

When creating the burial and erosion history for a particular well succession there are several factors to consider when defining the model inputs. More specifically, the thickness of sediment both deposited and removed by burial and erosion events can be constrained by several variables. Firstly, the thickness of formations present in the well section can be used as thickness inputs for each burial period, given that the stratigraphic ages of both the top and bottom of the formation are known and no erosion of the formation has taken place. Formations that extend beyond the bottom of the well can have a thickness estimate placed on them or can simply be ignored if the model begins at the point in time when the formation containing the deepest well sample began to be deposited (e.g. the burial history for Bounty-1 is taken as starting at deposition of the Scotty Mudstone, the lowermost member of the Matiri Formation and it is assumed that

the lower Maruia Formation would not affect the thermal history of the overlying sediments). Estimating the thickness of section that has been removed by erosion is more difficult as there is no way of knowing from the well section how much sediment has been removed. As discussed previously, the thickness of removed section can in fact be estimated from seismic mapping, the values for which match well to published estimates (King & Thrasher, 1996 and references therein), but this does require the availability of seismic reflection data. The well section can however reveal the time missing at the unconformity, with the younger age giving a clear idea of the point in time when erosion ceased and deposition resumed. It is harder to make estimates from the sedimentary section of the time when erosion started as the sediments of interest have been removed. For the Bounty-1 well, a value of 8 Ma is adopted for the start of erosion in Murchison Basin based on values published in the literature (Kamp & Green, 1990; Crowhurst et al., 2002), which were calculated from assessing the amount of heating and cooling required to account for the difference in the AFT ages and R_0 values. Ultimately, the amount of deposition and erosion has to allow the samples to (a) reach the temperature required so that enough annealing can take place to produce the measured AFT age, and (b), finish at a depth corresponding to their current position in the well. Bearing in mind that thickness must be rounded to the nearest 50 m (the maximum resolution of TQtec), a simple method of trial and error can be employed to adjust the thicknesses of units including those backstacked, as well as rates of erosion to match the predicted and observed AFT ages.

Thermal Modelling of Outcrop Samples

AFT analysis of outcrop samples from the Murchison Basin has yielded additional information about the thermal history of Murchison Basin sediments. The same modelling procedure that was used to analyse the Bounty-1 well samples can be used to model the AFT ages of the samples collected from outcrop, the locations of which are shown in Fig. 6. Six samples lie in close proximity to section line A-A', the cross-

section of which is shown in Fig. 7, and three of these (1116-12, -24 and -26) have been shown to have partial thermal overprinting by the presence of apatite grains which have AFT ages younger than the stratigraphic age of the sample horizons (Lee, 2013).

There are some key differences between the outcrop samples and the well samples that need to be taken into consideration in modelling. Firstly, all outcrop samples were collected from surface outcrop so have a relative depth of 0 m, unlike the Bounty-1 well samples, which each lie at a different depth in the well column. Each sample will therefore have to be modelled individually as all samples must finish at a depth of 0 m when the model ends at 0 Ma. The three samples with partial thermal overprinting also belong to three different formations and now reside at the surface because of contractional folding and faulting within the basin. This means that some adjustment will need to be made to the thicknesses of units removed by erosion as all samples need to finish at a depth of 0 m even though they will reach different maximum burial depths because of their different stratigraphic positions. Samples 1116-12 and -24 were also collected from outcrop on the basin margins and therefore are likely to have had a smaller thickness of sediment deposited above them compared with samples in the central basin. Thicknesses of units deposited have therefore been adjusted in the model.

To place better constraints on the burial history of the basin the AFT length distributions of the samples and the model output will be matched, rather than the age (as with the well samples). The reasoning for this is because the samples are unimodal and have a large range of single apatite grain ages so the central age is not representative of the whole sample and is therefore unsuitable to use in the modelling.

Sample 1116-24 (Brunner Coal Measures)

Sample 1116-24 was collected from an outcrop of Brunner Coal Measures (Maruia Formation) on the eastern margin of the basin along the Tiraumea River to the southeast of Tutaki. To produce the best match between the modelled and measured track length distributions, the

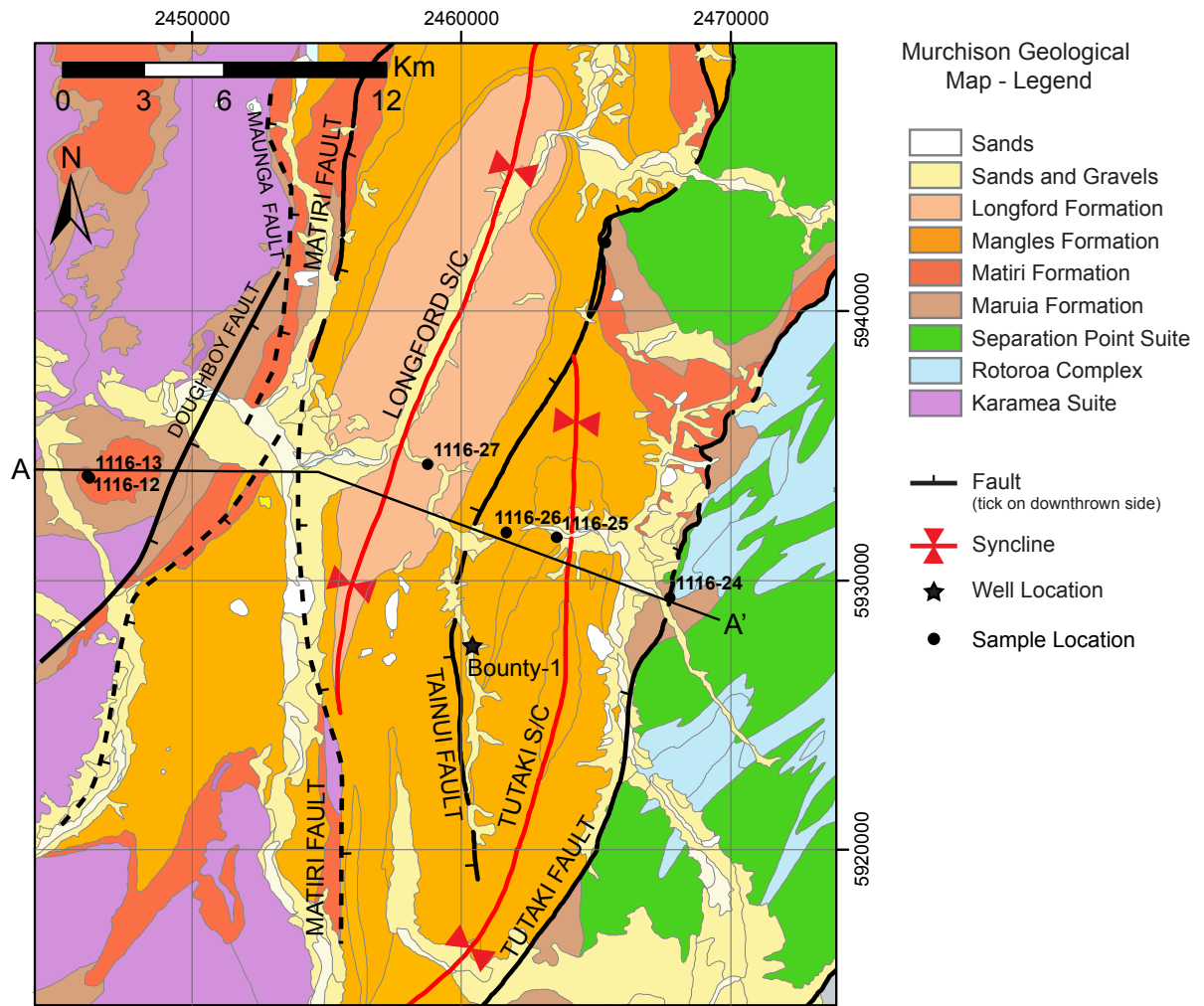


Figure 6. Map showing sample locations in Murchison Basin. The location of the Bounty-1 well is shown as the black star. The cross-section A-A' is shown in Fig. 7. Map data sourced from the Institute of Geological & Nuclear Sciences QMap project.

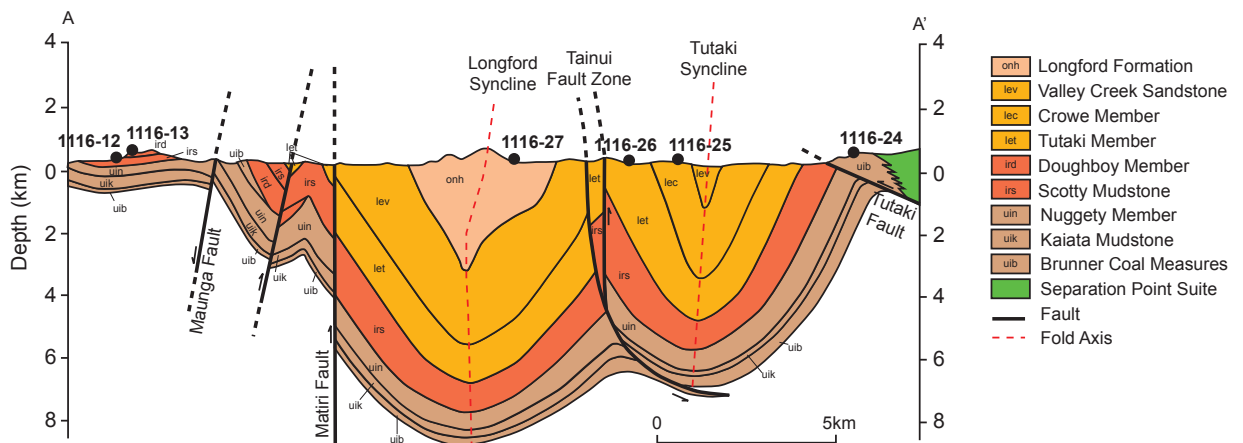


Figure 7. Cross-section A-A' for Murchison Basin. Approximate locations of samples are shown as black dots. Adapted from Lihou (1993) and Suggate (1984).

thicknesses of the units deposited as part of the sedimentary column were reduced to compensate for the sample's locality on the basin margin. Reducing the thicknesses to between 50 and 60% of their original thickness used in the Bounty-1 modelling produced the best match between predicted and observed data (given the model inputs have a maximum resolution of 50 m), the model inputs for which are shown in Table 16. A surface heat flow of 77 mWm^{-2} (determined from the modelling of the Bounty-1 well samples) was used as well as a surface temperature of $10 \text{ }^{\circ}\text{C}$ and a basement thermal conductivity of $3.0 \text{ Wm}^{-1}\text{K}^{-1}$. The measured and modelled track length distributions are shown in Fig. 8.

The modelled and measured track length distributions for sample 1116-24 have a relatively good match with their peak lengths, being $11 \mu\text{m}$ and $12 \mu\text{m}$ respectively. The main discrepancy between the two distributions is the lack of shorter tracks in the modelled distribution. This may have arisen because the composition of the apatite that had their confined tracks measured varies in chlorine content (crystals are fluorapatite) from the annealing model (which assumes a Durango composition), therefore affecting the annealing rate.

Sample 1116-12 (Scotty Mudstone Member)

Sample 1116-12 was collected from an outcrop of Scotty Mudstone (Matiri Formation) on the side of the Sphinx Mesa on the western margin of the basin. As with sample 1116-24, the thicknesses of the units were reduced, as this is a basin margin sample. In this case, reducing the thicknesses to 60 - 70% of the original thickness used in the Bounty-1 modelling produced the best match between the modelled and measured track length distributions (model inputs shown in Table 17). The measured and modelled track length distributions are shown in Fig. 9. The two length distributions match well apart from

Table 16. Burial history for 1116-24 that gives the best match between measured and modelled AFT length distributions.

Burial Start Time (Ma)	Burial End Time (Ma)	Thickness Deposited (m)	Thermal Conductivity ($\text{Wm}^{-1}\text{K}^{-1}$)	Equivalent Formation/Member
40	27	450	2.5	Brunner Coal - Scotty
27	24	200	2.5	Scotty/Doughboy
24	23	100	2.5	Scotty/Trig M
23	19	1000	3.4	Tutaki
19	14	100	3.2	Crowe/Valley Creek
14	9	1400	3.2	Longford
9	8	300	3.2	Rappahannock

Erosion Start Time (Ma)	Erosion End Time (Ma)	Thickness Eroded (m)
8	4	450
4	0	3100

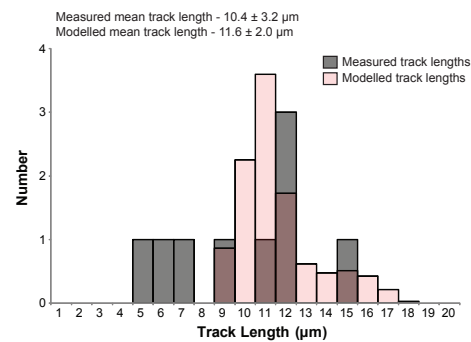


Figure 8. Measured and modelled apatite track length distributions for sample 1116-24 from the Brunner Coal Measures.

the high number of measured track lengths with a length of $8 \mu\text{m}$. As with sample 1116-24, this may reflect a difference in the chlorine content of the apatite in the sample (fluorapatite) resulting in a higher rate of annealing and shortening of tracks.

Sample 1116-26 (Tutaki Member)

Sample 1116-26 was collected from an outcrop of Tutaki Member sandstone on the south side of the Mangles - Tutaki Road. The sample originates from the central part of the basin rather than the margins (on the western limb of the Tutaki Syncline). Model inputs are detailed in Table 18 and the measured and modelled track length distributions are shown in Fig. 10.

Table 17. Burial history for sample 1116-12 that gives the best match between measured and modelled AFT length distributions.

Burial Start Time (Ma)	Burial End Time (Ma)	Thickness Deposited (m)	Thermal Conductivity ($\text{Wm}^{-1}\text{K}^{-1}$)	Equivalent Formation/Member
30	27	150	2.5	Brunner Coal - Scotty
27	24	250	2.5	Scotty/Doughboy
24	23	150	2.5	Scotty/Trig M
23	19	1100	3.4	Tutaki
19	14	150	3.2	Crowe/Valley Creek
14	9	1500	3.2	Longford
9	8	300	3.2	Rappahannock

Erosion Start Time (Ma)	Erosion End Time (Ma)	Thickness Eroded (m)
8	4	500
4	0	3100

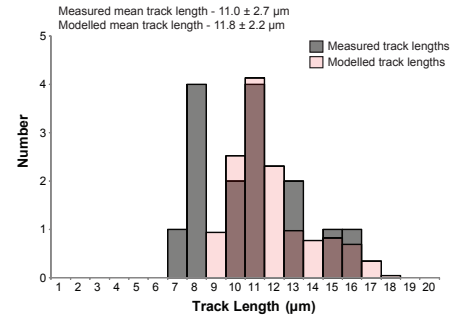


Figure 9. Measured and modelled apatite track length distributions for sample 1116-12 from the Scotty Mudstone Member.

Table 18. Burial history for sample 1116-26 that gives the best match between measured and modelled AFT length distributions.

Burial Start Time (Ma)	Burial End Time (Ma)	Thickness Deposited (m)	Thermal Conductivity ($\text{Wm}^{-1}\text{K}^{-1}$)	Equivalent Formation/Member
21	19	900	3.4	Tutaki
19	14	200	3.2	Crowe/Valley Creek
14	9	2500	3.2	Longford
9	8	500	3.2	Rappahannock

Erosion Start Time (Ma)	Erosion End Time (Ma)	Thickness Eroded (m)
8	4	800
4	0	3300

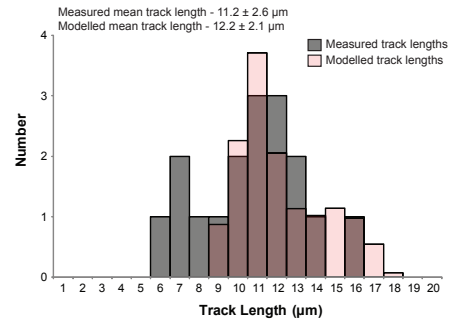


Figure 10. Measured and modelled apatite track length distributions for sample 1116-26 from the Tutaki Member.

Sample 1116-26 has the same pattern as for the previous two samples with a good match between the distributions apart from the presence of shorter measured track lengths. To increase the number of shorter tracks in the modelled distribution, adjustments would need to be made to either the burial history or the thermal properties in the model. Surface heat flow and sediment thermal conductivities are both constrained in the Bounty-1 modelling so are not changed for outcrop modelling. Increasing the thicknesses of the units would result in the samples being buried deeper and reaching a higher temperature (resulting in shortening

of tracks), however this results in the longer track lengths disappearing in the modelled distribution. Also, the model inputs for sample 1116-26 already incorporate the maximum unit thicknesses (defined by Bounty-1 modelling) so could not be increased further.

The measured track length distributions of these three samples can be compared with distributions of track length measured by Gibson (1993) (Fig. 11), who collected outcrop samples from the same members. The three Gibson (1993) samples were selected based on their outcrop location being close to the

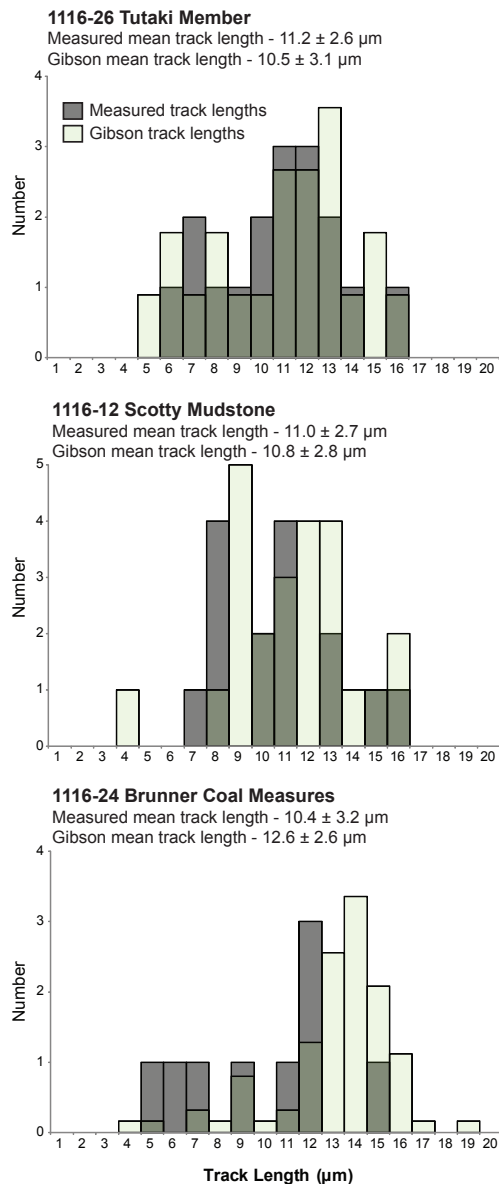


Figure 11. Measured track length distributions from this study and from Gibson (1993). Gibson (1993) samples plotted are HR2-22 (Brunner Coal Measures), HR2-37 (Scotty Mudstone) and HR2-17 (Tutaki Member).

outcrops from which samples 1116-12, -24 and -26 were obtained. The distributions for samples 1116-26 and HR2-17 from the Tutaki Member display a very good match with both distributions containing long (14 - 16 μm) and short (5 - 10 μm) tracks. The distributions for the Scotty Mudstone samples (1116-12 and HR2-37) have a reasonable match, although the tracks from 1116-12 may on average be marginally shorter than in sample HR2-37. The Brunner Coal Measures samples have some differences, mainly the high number of tracks with 13 - 15 μm lengths in the Gibson (1993) distribution. In her forward modelling of the track length

distributions, Gibson includes a period of cooling from 35 to 25 Ma to model estimates of post-depositional maximum paleotemperature. As her sample of Brunner Coal Measures HR2-22 originated from an outcrop only a few hundred metres from sample 1116-24, this period of cooling will be incorporated into the burial history for this sample to see if it has any impact on the track length distribution. The revised burial history used as a model input is outlined in Table 19, with all other model parameters remaining the same. An arbitrary value of 200 m is used as the amount of section removed by erosion between 35 and 25 Ma.

The measured and modelled track length distributions for sample 1116-24 are shown in Fig. 12. Adding a period of cooling between 35 and 25 Ma has produced a better match between the measured and modelled distribution, which supports the original theory put forward by Gibson (1993) that the eastern margin of the basin underwent a period of cooling whilst subsidence and burial was taking place in the central and western regions.

Hydrocarbon Prospectivity in southern Taranaki and Murchison basins

Some 10 wells have been drilled in southern Taranaki Basin to explore for hydrocarbon resources over the last few decades. The majority of wells targeted the Eocene Pakawau Coal Measures and Kapuni Group in addition to stratigraphically higher formations such as the Middle Miocene Moki Formation. The Paleocene - Eocene formations are productive in the Maui Field directly to the north of the Southern Inversion Zone and it was originally hoped that similar stratigraphic traps would be present in more southern parts of the basin (PR 677). For example, the three-way closure within Fresne-1, Surville-1 and North Tasman-1 structures, amongst others, were anticipated to contain hydrocarbons. All three wells targeted the Pakawau Coal Measures, which proved to be water bearing in each case, indicating lack of charge (a water drive is thought to have forced

Table 19. Revised burial history for sample 1116-24, including a period of erosion (cooling) between 35 and 25Ma.

Burial Start Time (Ma)	Burial End Time (Ma)	Thickness Deposited (m)	Thermal Conductivity ($\text{Wm}^{-1}\text{K}^{-1}$)	Equivalent Formation/Member
40	35	450	2.5	Brunner Coal - Scotty
25	24	200	2.5	Scotty/Doughboy
24	23	100	2.5	Scotty/Trig M
23	19	1000	3.4	Tutaki
19	14	100	3.2	Crowe/Valley Creek
14	9	1400	3.2	Longford
9	8	300	3.2	Rappahannock

Erosion Start Time (Ma)	Erosion End Time (Ma)	Thickness Eroded (m)
35	25	200
8	4	450
4	0	2900

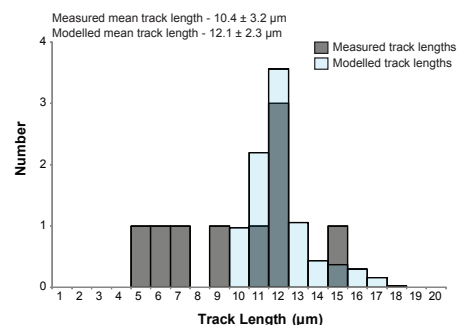


Figure 12. Measured and modelled track length distributions for sample 1116-24 from the Brunner Coal Measures. Modelled distribution incorporates a cooling period from 35 - 25 Ma, as shown in Table 19.

the hydrocarbons to migrate elsewhere). This migration of hydrocarbons must have taken place prior to the formation of the traps in Fresne-1 and Surville-1. In North Tasman-1, the migration resulted in complete loss of hydrocarbons through the poorly consolidated and reasonably permeable cap rock of the Abel Head Formation.

Oil and gas shows are relatively common in the Murchison Basin in the vicinity of Bounty-1, however it has not been commercially exploited. Oil and gas have probably escaped through the heavily fractured successions lying above the Maruia Formation source rocks.

Maximum Paleotemperature and Duration of Heating

Hydrocarbon maturation is a function of both time and temperature. To assess the degree of catagenesis that has taken place in source rocks, both the maximum temperature and the duration the source rocks have experienced maximum temperatures are required to be known. Modelling outputs from FTage allow the heating duration to be established for all three Taranaki Basin wells and for the Bounty-1 well using the time-temperature profile, which assesses if there was the potential for hydrocarbons to mature during the basin's burial history (Fig. 13).

The time-temperature profiles were plotted using the predicted maximum temperature values of the deepest well sample modelled at 400,000-year increments. Presently, significant oil generation generally occurs between 100 and 150 °C (with gas formation taking place at temperatures up to 225 °C) (Bjørlykke, 2010) over geological periods longer than 1 million years. The exact temperatures required for oil formation have been linked to the age of the sediments and the geothermal gradient, with a general rule of thumb being that younger sediments require higher temperatures to begin oil generation (North, 1994 and references therein) as well as kerogen type. Type III kerogen is the most likely form of kerogen produced in the Maruia Formation rocks, which is most commonly associated with coal measures.

The deepest sample from Fresne-1 (8694-14) originates from the Pakawau Group, which are considered to be the source rocks for this particular region. The time-temperature profile in Fig. 13 is therefore a true reflection of the maturity of the source rocks that experienced temperatures above 100 °C for 8.4 million years. Residing at these temperatures over this period would allow significant maturation of the kerogen in the source rocks to take place resulting in the production of oil.

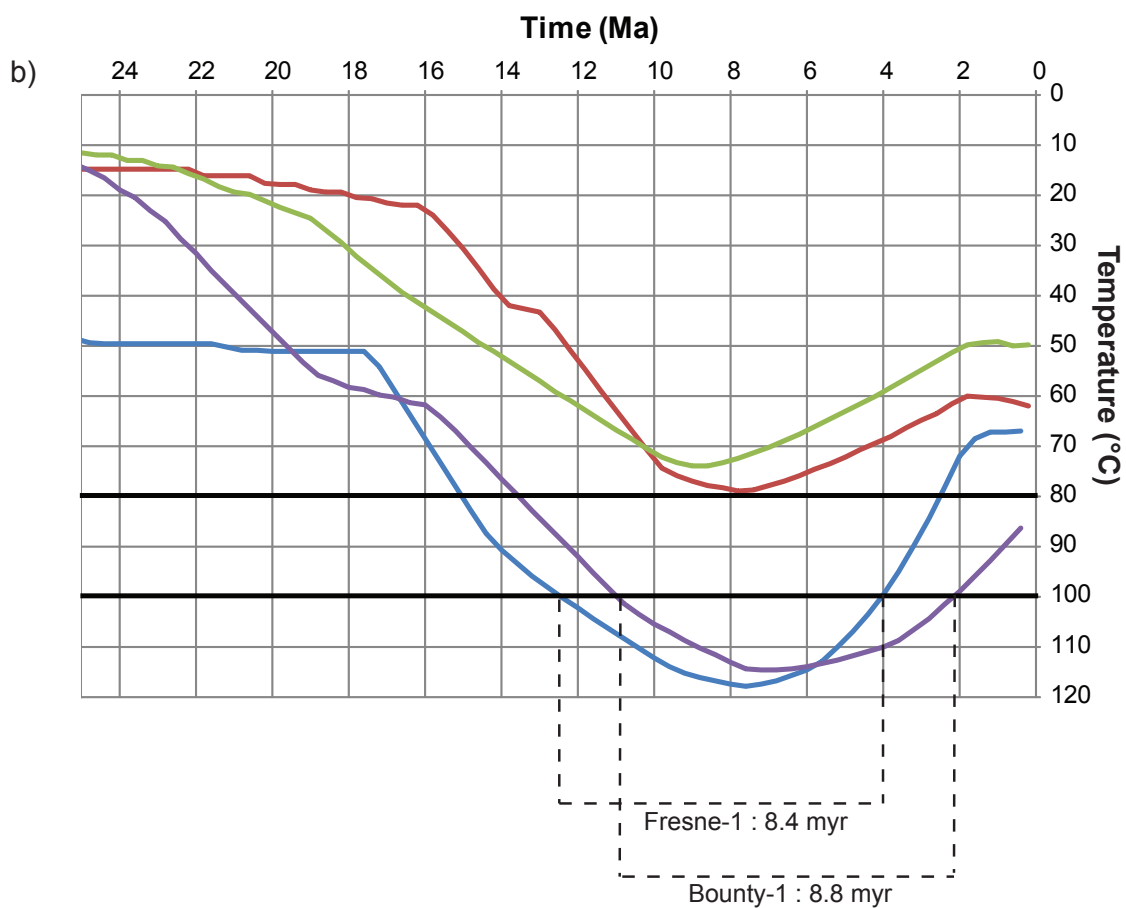
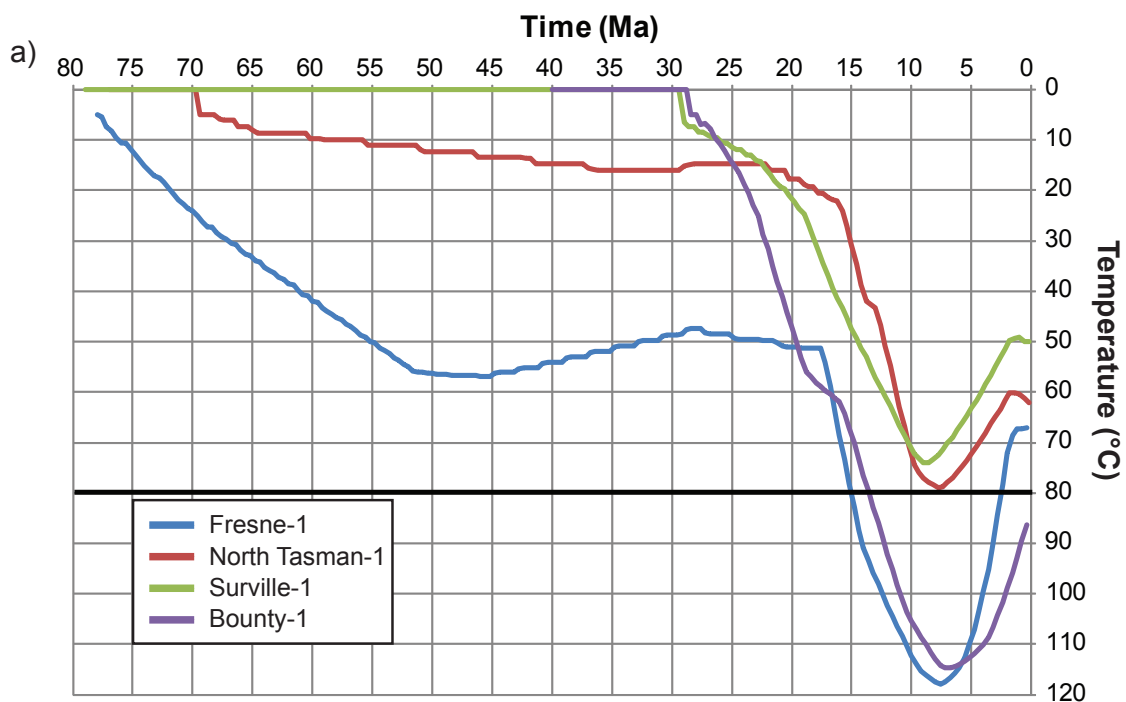


Figure 13. Time-temperature profiles plotted from the FTage output for Fresne-1, North Tasman-1, Surville-1 and Bounty-1 over timescales of a) 80 - 0 Ma, and b) 25 - 0 Ma. The black horizontal line at 80 °C indicates the temperature at the top of the oil window. Figure 13b shows the time spent in the oil generation window given for each well. A second black line at 100 °C shows the starting temperature for significant maturation.

The Bounty-1 drilling did not reach the Maruia Formation source rocks and instead terminated in the overlying Matiri Formation so the time-temperature profile shown in Fig. 13 is not a true reflection of the temperatures experienced by the deeper source rocks. The Matiri Formation sample (HR2-14) did however reside at temperatures over 100 °C for 8.8 million years, indicating that maturation would have taken place in the underlying Maruia Formation. As with Fresne-1, it is highly likely that oil would have been produced in these source rocks as the kerogen formed in the Maruia Formation sediments would have been sitting at a high enough temperature for several million years.

Time-Temperature Index and Vitrinite Reflectance

The relationship between time and temperature can be expressed in terms of a time-temperature index (TTI) value, as first defined by Lopatin (1971) and Waples (1980). The TTI is calculated based on the amount of time spent at each 10 °C temperature increment within the oil-producing window by using the formula:

$$\text{Equation 3: } \text{TTI} = \sum (\text{ti})(\text{rn})$$

where t_i is the time in millions of years spent in the i th temperature interval, r is the factor by which the maturation rate increase with each 10 °C increase in temperature (a value of 2 is generally used, assuming the reaction rate doubles for every 10 °C increase) and n is the index value for the temperature interval. The interval 100 - 110 °C is arbitrarily given an 'n' value of 0, consequently the value for 90 - 100 °C is -1, +1 for 110 - 120 °C and so on. The TTI value gives an indication of the thermal maturity of the oil, first defined by Waples (1980) and shown in Table 20.

Table 20. Important stages of oil generation and the corresponding TTI and Ro values (adapted from Waples, 1980).

Stage	TTI	R _o
Onset of oil generation	15	0.65
Peak of oil generation	75	1.00
End of oil generation	160	1.30

Both TTI and Ro (vitrinite reflectance) values are produced as an output from FTage and therefore can be used to assess the potential for oil maturation at each of the wells. Vitrinite reflectance offers an additional thermal indicator that can provide information regarding paleotemperature and the potential for hydrocarbon maturation (given that it is both time and temperature dependent). TTI and vitrinite reflectance are commonly used in conjunction to assess maturation potential as both provide a numerical window for oil and gas generation. The outputs from FTage for the deepest sample modelled in each well are shown in Table 21.

Table 21. TTI and Ro values calculated in FTage for the deepest samples in Fresne-1, North Tasman-1, Surville-1 and Bounty-1.

Well	TTI	R _o
Fresne-1	16.88	0.82
North Tasman-1	2.19	0.53
Surville-1	0.94	0.44
Bounty-1	16.00	0.81

Of the four wells, only Fresne-1 and Bounty-1 have TTI and Ro values that fall within the oil generation window. That said, their TTI values are very close to the bottom threshold required for oil formation with the limited amount of time spent in the 80 - 120 °C temperature range being the reason for their values being so low. The validity of these TTI values depends strongly on the basin burial history model as this directly determines the time-temperature profiles required for the TTI calculation. A good level of confidence can be placed in the TTI values for both Fresne-1 and Bounty-1 as their burial histories were created by correlation of several AFT data points over a considerable depth range. The vitrinite reflectance values for Bounty-1 and Fresne-1 are also in the onset of oil generation window but as with the TTI values, are at the low end of the spectrum simply because the sediments did not remain at their peak temperature for a substantial period.

Timing of Inversion and Maturation

The thermal maturation indicators used in this study to assess the oil generation potential in Fresne-1 and Bounty-1 all suggest that the deepest sediment samples were certainly subjected to the necessary temperatures for a period long enough for oil generation to occur. As no oil remains in the reservoir horizons of either well, it is logical to assume that the oil generation occurred prior to the formation of the structural traps. Figure 14 shows a timeline of events relevant to the generation and trapping of oil in both Fresne-1 and Bounty-1 structures. The top two lines show the period during which source rocks in Fresne-1 and Bounty-1 were in the oil producing window at temperatures over 100 °C. The blue dashed line represents the approximate timing of uplift of the Pakawau sub-basin, which is bounded to the east by the Wakamarama Fault and to the west by the Kahurangi Fault and contains the Wakamarama Anticline into which Fresne-1 was drilled (Figure 3.7a in King & Thrasher, 1996). Uplift on the Wakamarama Anticline is thought to have occurred after the Middle Miocene, based on the presence of folded and uplifted Early - Middle Miocene units preserved on the flanks of the structure (King & Thrasher, 1996). Despite uplift occurring prior to the source rocks at Fresne-1 reaching their maximum paleotemperature, secondary migration must have taken place prior to anticlinal structural traps forming as the

Pakawau Coal Measures are now water bearing. Oil staining along fractures in the overlying Cobden and Abel Head formations indicates that these fractures acted as conduits allowing secondary migration away from the Pakawau Group rocks. Movement on the Wakamarama Fault may also have provided a pathway for oil to migrate as fault wall rocks can become unstable and permeable after reactivation.

The structural development in the Murchison Basin follows a similar regime with previous normal faults having been reactivated as reverse faults during the late Neogene. The anticline structure that Bounty-1 penetrates (the Blackwater Anticline) has quite a different geometry to that of the Wakamarama Anticline, with limbs that are very steeply dipping and a reverse fault to the west (Tainui Fault). Reverse movement on the Tainui Fault has in fact removed almost all of the Blackwater Anticline (Lihou, 1993) and has resulted in a significantly thickened section of the Matiri Formation being present in the Bounty-1 well (Fig. 5). Hydrocarbon migration at Bounty-1 is predominantly attributed to extensive fracturing and poor reservoir characteristics (indicated by low porosity) but could also be a result of the structural development of the basin. As with the Wakamarama Fault, the Tainui Fault was reactivated during the late Neogene, opening up a conduit for oil to escape having matured in the underlying Maruia Formation.

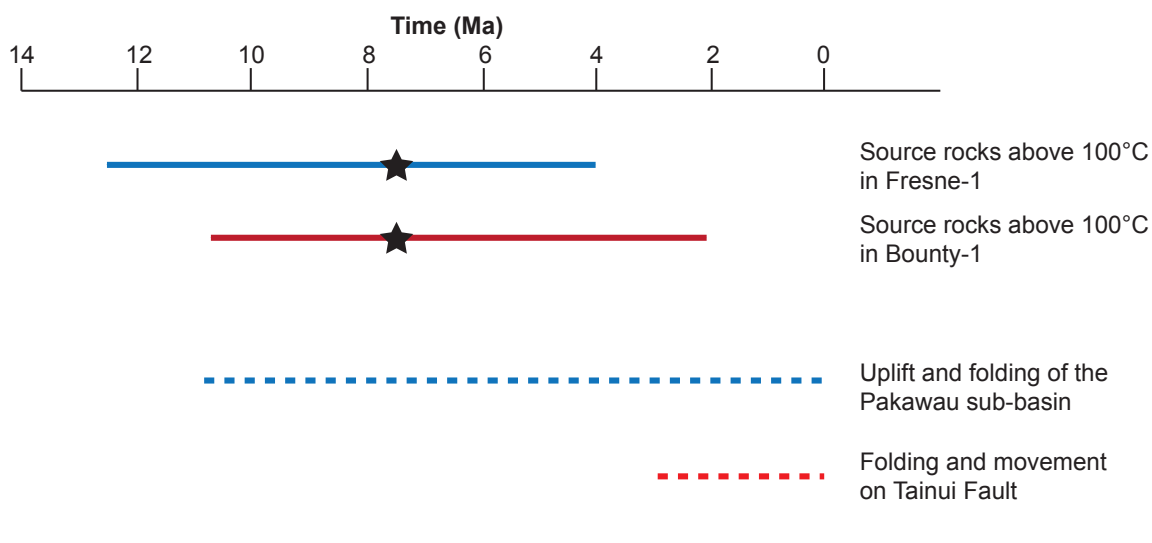


Figure 14. Timeline of oil maturation and the formation of key structures in the region of Fresne-1 and Bounty-1 wells. Black stars show the timing of maximum paleotemperature.

Summary

Numerical thermal modelling of sedimentary successions for drill hole stratigraphy can yield important information regarding the deformation of host basins. To create a comprehensive thermal history for a succession, several parameters being inputs to a numerical model (TQtec and FTage) need to be constrained. Four well successions in Southern Taranaki Basin, each having a detailed well stratigraphy, were used in numerical modelling to constrain the surface heat flow at the time of maximum burial by comparison of predicted with observed AFT ages for samples. The amount of section removed by erosion at the Late Miocene unconformity (Taranaki Basin) was estimated for each well by seismic mapping of a continuous Oligocene reflector (Jager, 2012). Erosion amounts varied from ~1100 m at North Tasman-1 to over 2600 m at Fresne-1 and compared well with estimates made by previous authors. These values have been used to estimate surface heat flow in the basin through application of a numerical model. The best match between predicted and observed fission track ages in the Fresne-1 succession was produced using a surface heat flow value of $79 \pm 6 \text{ mWm}^{-2}$, which is higher than the present day value of $70 \pm 12 \text{ mWm}^{-2}$ (Funnell et al., 1996) but has probably been reduced since the Late Miocene as a result of the cooling effect caused by the emplacement of the subducted Pacific oceanic slab underneath the region (Furlong and Kamp 2009). The modelling results for North Tasman-1 resulted in a maximum surface heat flow value of 82 mWm^{-2} and Surville-1 gave a minimum value of 73 mWm^{-2} .

These values for paleo-surface heat flow have been utilised to constrain a surface heat flow value for the Bounty-1 well succession in Murchison Basin for which the late burial and erosion history are poorly constrained. The value of 77 mWm^{-2} was used in the Bounty-1 model and the amounts of burial and erosion were adjusted to achieve a match between the measured and predicted AFT ages. The burial history required to produce an acceptable match placed constraints on the timing of uplift (starting at 10 Ma), timing of erosion (starting at

8 Ma) and the amount of section removed at the Late Miocene unconformity (2550 m). To better understand the thermal history of Murchison Basin, burial histories for key outcrop samples have been created to produce modelled track length distributions. These were then matched to the measured track length distributions for the outcrop samples to further constrain the burial history of the basin.

Having a more comprehensive understanding of the thermal history of Southern Taranaki and Murchison basins also allows for a better evaluation of the hydrocarbon prospectivity of the region. Model outputs of FTage include time-temperature index values and vitrinite reflectance data, both of which are time and temperature controlled. Despite all four wells investigated reaching the oil window at some point in their history (between temperature of $60 \text{ }^{\circ}\text{C}$ and $120 \text{ }^{\circ}\text{C}$), no well section containing source rocks spent enough time at high enough temperatures for hydrocarbons to be produced in significant volumes. The absence of significant quantities of oil in these drill hole successions is also attributed to the timing of the heating as hydrocarbon maturation in both southern Taranaki and Murchison wells took place prior to the formation of structural traps.

Acknowledgements

We acknowledge the New Zealand Foundation for Research Science and Technology, Ministry of Business Innovation and Employment (Contract UOW X0902) for research funding. Also OMV (New Zealand) Ltd for their research funding support. We acknowledge Betty-Ann Kamp for cartographic assistance.

References

- Armstrong, P.A., Chapman, D.S., Funnell, R.H., Allis, R.G., Kamp, P.J.J. (1996). Thermal Modeling and Hydrocarbon Generation in an Active-Margin Basin: Taranaki Basin, New Zealand. *AAPG Bulletin*, 80, p. 1216-1241.
- Bjørlykke, K. (2010). *Petroleum Geoscience: From Sedimentary Environments to Rock Physics*. Springer-Verlag Berlin Heidelberg, 508 p.
- Carlson, C.D. (1990). Mechanisms and kinetics of apatite fission-track annealing. *American Mineralogist*, 75, p. 1120-1139.
- Crowhurst, P.V., Green, P.F., Kamp, P.J.J. (2002). Appraisal of (U-Th)/He apatite thermochronology as a thermal history tool for hydrocarbon exploration: An example from the Taranaki Basin, New Zealand. *AAPG Bulletin*, 86, p. 1801-1819.
- Ellyard, T., Beattie, B. (1990). Inversion structures and hydrocarbon potential of the Southern Taranaki Basin. In: 1989 New Zealand Oil Exploration Conference proceedings. Ministry of Commerce, Wellington, p. 259-271.
- Funnell, R.H., Chapman, D.S., Allis, R.G., Armstrong, P.A. (1996). Thermal state of the Taranaki Basin, New Zealand. *Journal of Geophysical Research*, 101, p. 25197-25215.
- Furlong, K.P., Guzowski, C. (2000). Thermal Rheological Evolution of the Franciscan Crust: Implications for Earthquake Processes. Proceedings of the 3rd Conference on Tectonic Problems of the San Andreas Fault System, eds. G. Bokelmann and R.L. Kovach, Stanford Univ. Press, p 112-127.
- Furlong, K.P. & Kamp, P.J.J. (2009). The lithospheric geodynamics of plate boundary transpression in New Zealand: Initiating and emplacing subduction along the Hikurangi margin, and the tectonic evolution of the Alpine Fault system. *Tectonophysics*, 474(3-4), 449-462.
- Gibson, H.J. (1993). *The Tectonic and Thermal Evolution of the Murchison Basin, New Zealand: An Apatite Fission Track Study*. Unpublished MSc thesis, University of Melbourne, Australia.
- Green, P.F., Duddy, I.R., Gleadlow, A.J.W., Tingate, P.R., Laslett, G.M. (1986). Thermal Annealing of Fission Tracks in Apatite 1. A Qualitative Description. *Chemical Geology*, 59, p. 237-253.
- Jager, K.G. (2012). *Seismic Stratigraphy of the Neogene Succession in Southern Taranaki Basin, New Zealand*. Unpublished MSc thesis, University of Waikato, Hamilton.
- Kamp, P.J.J., Green, P.F. (1990). Thermal and Tectonic History of Selected Taranaki Basin (New Zealand) Wells Assessed by Apatite Fission Track Analysis. *AAPG Bulletin*, 74, p. 1401-1419.
- Ketcham, R.A. (2005). Forward and Inverse Modeling of Low-Temperature Thermochronometry Data. *Reviews in Mineralogy and Geochemistry*, 58, p. 275-314.
- King, P.R., Thrasher, G.P. (1996). *Cretaceous-Cenozoic geology and petroleum systems of the Taranaki Basin, New Zealand*. Institute of Geological and Nuclear Sciences monograph 13. 243p + 6 enclosures. Lower Hutt, New Zealand. Institute of Geological and Nuclear Sciences Limited.
- Knox, G.J. (1982). Taranaki Basin, structural style and tectonic setting. *New Zealand Journal of Geology and Geophysics*, 25, p. 125-140.
- Laslett, G.M., Green, P.F., Duddy, I.R., Gleadlow, A.J.W. (1987). Thermal Annealing of Fission Tracks in Apatite 2. A Quantitative Analysis. *Chemical Geology*, 65, p. 1-13.
- Legg, M.J. (2010). *The tectonic and thermal evolution of Hawke's Bay Basin, New Zealand*. Unpublished MSc thesis, Pennsylvania State University.
- Lee, S. (2013). *Provenance and Thermal History of the Cenozoic Murchison Basin, Westland, New Zealand*. Unpublished PhD thesis, University of Waikato, Hamilton.
- Lihou, J.C. (1993). The structure and deformation of the Murchison Basin, South Island, New Zealand. *New Zealand Journal of Geology and Geophysics*, 36, p. 95-105.
- Lopatin, N.V. (1971). Temperature and geologic time as factors in coalification. *Izvestiya Akademiya Nauk SSSR*, 3, p. 95-106 (in Russian).
- North, F.K. (1994). *Petroleum Geology*, 2nd Edition. Chapman & Hall, London, UK.
- Strogen, D.P. (compiler) (2011). *Paleogeographic synthesis of the Taranaki Basin and surrounds*. GNS Science Report, 2010/53.

- Suggate, R.P. (1984). Sheet M29AC – Mangles Valley. Geological map of New Zealand 1:50 000. Wellington, New Zealand. Department of Scientific and Industrial Research.
- Townend, J. (1999). Heat flow through the West Coast, South Island, New Zealand. *New Zealand Journal of Geology and Geophysics*, 42, p. 21-31.
- Waples, D.W. (1980). Time and temperature in petroleum formation: application of Lopatin's method to petroleum exploration. *AAPG Bulletin*, 64, p. 916-926.
- Willett, S.D. (1997). Inverse modelling of annealing of fission tracks in apatite 1: a controlled random search method. *American Journal of Science*, 297, p. 939-969.